PENSOFT.

SENCKENBERG
world of biodiversity

Leibniz
Leibniz
Association

Diversity and phylogeny of the extinct wasp subfamily Lancepyrinae (Hymenoptera, Bethylidae) revealed by mid-Cretaceous Burmese amber

Manuel Brazidec[1,2], Frédéric Legendre[3], Vincent Perrichot[1]

1 *Univ. Rennes, CNRS, Géosciences Rennes, UMR 6118, 35000 Rennes, France*

2 *State Key Laboratory of Palaeobiology and Stratigraphy, Nanjing Institute of Geology and Palaeontology and Center for Excellence in Life and Paleoenvironment, Chinese Academy of Sciences, 39 East Beijing Road, Nanjing 210008, China*

3 *Institut de Systématique, Évolution, Biodiversité (ISYEB), Muséum national d'Histoire naturelle, CNRS, Sorbonne Université, EPHE, Université des Antilles, CP50, 57, rue Cuvier, 75005 Paris, France*

https://zoobank.org/0C2444B0-ECFB-4A22-ACF6-F2ACEC0DDCDF

Corresponding author: Manuel Brazidec (manuel.brazidec@gmail.com)

Citation: Brazidec M, Legendre F, Perrichot V (2023) Diversity and phylogeny of the extinct wasp subfamily Lancepyrinae (Hymenoptera, Bethylidae) revealed by mid-Cretaceous Burmese amber. Arthropod Systematics & Phylogeny 81: 345–369. https://doi.org/10.3897/asp.81.e96737

Abstract

The Lancepyrinae are an extinct subfamily of Bethylidae known exclusively from Cretaceous amber deposits of Lebanon, Spain, Taimyr and Myanmar. In this study, we describe and illustrate four new genera and five new species of lancepyrine wasps from the Albian of Hkamti and late Albian-early Cenomanian of Kachin (Myanmar): *Azepyris delamarrei* **gen. et sp. nov.**, *Burmapyris ohmkuhnlei* **sp. nov.**, *Gwesped groehni* **gen. et sp. nov.**, *Paralanceis chotardi* **gen. et sp. nov.** and *Yunbayin rossei* **gen. et sp. nov.** These taxa not only highlight the taxonomic diversity of the Lancepyrinae during the mid-Cretaceous but they also reveal the morphological disparity of the subfamily. To establish the phylogenetic relationships of these fossils and to check the monophyly of the Lancepyrinae, we add them to a pre-existing morphological matrix and perform a cladistic analysis. We retrieve the subfamily as poorly supported yet monophyletic, with the newly described taxa deeply nested in it. A key to the genera of Lancepyrinae is provided. Finally, we erect the subfamily Cretabythinae **subfam. nov.** for the genera *Cretabythus* Evans, 1973, *Holopsenelliscus* Engel, 2019 and *Megalopsenella* Jouault et al., 2020 as no taxonomic treatment has been provided for these taxa after the transfer of *Holopsenella* Engel et al., 2016 as Aculeata *incertae sedis*.

Keywords

Chrysidoidea, Bethylidae, fossil record, taxonomy, Kachin amber, Hkamti amber

1.   Introduction

With no less than 2900 extant species, whose biology is assumed to be parasitic on lepidopteran and coleopteran larvae, the Bethylidae are the largest family within the Chrysidoidea (Evans 1964; Azevedo et al. 2018, 2019). This great diversity is also witnessed through geological times, with more than 100 species documented from compressions, copal and amber deposits ranging from the Holocene to the Early Cretaceous (e.g., Martynova et al. 2019; Colombo and Azevedo 2021; Colombo et al. 2021a, 2021b). However, despite a fossil record spanning a 130

million year-long evolutionary history, the corresponding geological periods have been studied differently. Until the 2010s, the majority of species was described from Cenozoic deposits (lower Eocene French, upper Eocene Baltic, Miocene Dominican ambers) whereas the renewed interest in Cretaceous Bethylidae is more recent (e.g., Azevedo and Azar 2012; Ortega-Blanco and Engel 2013; McKellar and Engel 2014; Jouault et al. 2020). These studies have highlighted a fairly high diversity of fossil bethylids—especially from the Cretaceous deposits of Myanmar—and have revealed the existence of extinct lineages such as the Lancepyrinae. Known exclusively from the Cretaceous, this subfamily was erected in 2012 based on an individual from Early Cretaceous Lebanese amber with a curious combination of characters of Bethylinae, Pristocerinae and Epyrinae (Azevedo and Azar 2012). Named *Lancepyris* Azevedo and Azar, 2012, it was, and still is, the oldest known bethylid wasp. Subsequently, a few newly or previously described taxa have been assigned to this subfamily: from Albian Spanish amber (Ortega-Blanco and Engel 2013), Cenomanian Burmese amber (Engel et al. 2016; Jouault et al. 2021), and from Santonian Taimyr amber (Evans 1973, transferred to Lancepyrinae by Engel et al. 2016). With the presence of Lancepyrinae revealed in Burmese amber, a paleobiogeographic scenario was proposed for the Bethylidae, with an origin dating back to the earliest Cretaceous and more probably to the Late Jurassic, before the Burma Terrane broke away from East Gondwana (Jouault et al. 2021). The subfamily was also studied phylogenetically and, interestingly, was not retrieved as the sister-group of other bethylids, a position occupied by Bethylinae (Azevedo and Azar 2012), Lancepyrinae being sister to the remaining subfamilies. A similar position was found by Colombo et al. (2020), but with the Holopsenellinae diverging first, while Jouault et al. (2021) grouped them with Protopristocerinae to form a clade sister to (Scleroderminae + (Epyrinae + (Pristocerinae + Mesitiinae))). The exact position of Lancepyrinae is yet to be determined, but authors agree that they are not the sister-group of the other bethylids. This implies that at least two subfamilies of Bethylidae had already diverged by the Early Cretaceous and provides paths of inquiry and calibration points for future analyses that aim to estimate divergence times of bethylid lineages.

In this paper, we report and describe various new genera and species of Lancepyrinae from mid-Cretaceous Burmese amber, and we explore the monophyly of the subfamily. We also present an illustrated key to the genera of Lancepyrinae.

2. Material and methods

2.1. Amber specimens

Three of the amber pieces studied herein originated from the deposits of Noije Bum, in the Hukawng Valley of Kachin State, northern Myanmar (see map in Grimal-

di et al. 2002: fig. 1). Radiometric data and taphonomic analysis of pholadids established an early Cenomanian age (98.79 ± 0.62 Ma) for Kachin amber, based on zircons from volcanic clasts found within the amber-bearing sediments (Shi et al. 2012; Smith and Ross 2017). Some ammonites found in the amber-bearing bed and within amber corroborate a late Albian-early Cenomanian age (Cruickshank and Ko 2003; Yu et al. 2019). Three other amber pieces originated from the deposits of Hkamti site, Hkamti district, Sagaing Region, Myanmar (see map in Zheng et al. 2018: supplementary figure 2). Radiometric data established an early Albian age (109.7 ± 0.4 Ma) for Hkamti amber, whose biota is still largely unknown.

Specimen IGR.BU-062 was acquired by one of us (V.P.). Specimens IGR.BU-060 and IGR.BU-063 were donated by Dr Christoph Öhm-Kühnle (Herrenberg, Germany) and specimen IGR.BU-061 by Corentin Jouault (MNHN, Paris, France) to the Geology Department and Museum of the University of Rennes, France (**IGR**). This material is housed in the amber collection of the IGR. Specimen GPIH.5058 (CCGG nº11341) was loaned for study by Carsten Gröhn (Glinde, Germany) and is deposited in the amber collection of the Leibniz Institute for the Analysis of Biodiversity Change, Hamburg, Germany (**GPIH**, Carsten Gröhn coll. CCGG). Specimen SNHM-6001 was loaned by Patrick Müller (Zweibrücken, Germany) and is deposited in the paleontological collection of the Staatliches Naturhistorisches Museum Braunschweig, Germany (**SNHM**).

2.2. Examination and imaging

The amber pieces have been trimmed and polished to facilitate the observation of the specimens, using thin silicon carbide papers on a grinder polisher (Buehler MetaServ 3000). Observations and photographs were conducted with a Leica DMC4500 camera attached to a Leica M205C stereomicroscope. All images are digitally stacked photomicrographic composites of several focal planes, which were obtained using Helicon Focus 6.7. Adobe Illustrator CC2019 and Photoshop CC2019 software were used to compose the figures and ImageJ 1.53 for measurements (Schneider et al. 2012). Habitus or details of the body have been redrawn digitally from drawings made with a camera lucida attached to the stereomicroscope.

2.3. Terminology and measurements

The description of the characters follows the nomenclature of Lanes et al. (2020) except the fore wing venation that follows Azevedo et al. (2018) and the description of surface sculpturing that follows Harris (1979). Abbreviations of wing veins and cells are used as follows: **[C]** = costal cell; **[R]** = radial cell; **[1Cu]** = first cubital cell; **[1R1]** = first radial cell; **[1M]** = first medial cell; **[2Cu]** = second cubital cell; **[2R1]** = second radial cell; **C** = costal

vein; **Sc+R** = subcostal + radial vein; **M+Cu** = median + cubital vein; **A** = anal vein; **1Rs** = first abscissa of radial sector; **1M** = first abscissa of median vein; **1Cu** = first abscissa of cubital vein; **2Cu** = second abscissa of cubital vein; **m-cu** = medio-cubital vein; **cu-a** = cubito-anal vein; **Rs+M** = radial sector + median vein; **2r-rs&Rs** = second radial cross and radial sector; **R1** = poststigmal abscissa of radial 1 vein. Main measurements and indices used are as follows: **DAO** = maximum diameter of anterior ocellus; **HE** = maximum width of eye in lateral view; **LFW** = maximum length of fore wing from apex of axillary sclerite to wing apex; **LH** = length of head capsule excluding mandibles, measured from posteriormost point of vertex to anteriormost point of clypeus; **OOL** = ocello-ocular line, minimum length from posterior ocellus to ocular margin; **VOL** = vertex-ocular line, minimum length from vertex posterior margin to posteriormost eye margin, measured in lateral view; **WF** = width of frons measured in dorsal view; **WH** = width of head measured immediately behind eyes in dorsal view; **WOT** = maximum width of ocellar triangle, measured in dorsal view. This published work and its new nomenclatural acts are registered in ZooBank with the following LSID (reference): urn:lsid:zoobank. org:pub:0C2444B0-ECFB-4A22-ACF6-F2ACEC0D-DCDF

2.4. Phylogenetic analysis

In order to test the monophyly of the Lancepyrinae, all genera considered as belonging to this subfamily—either in this contribution or in previous works (i.e., Azevedo and Azar 2012; Ortega-Blanco and Engel 2013; Engel et al. 2016; Azevedo et al. 2018; Jouault et al. 2021)—were added to the matrix of Colombo et al. (2020: table 2), initially containing 22 taxa and a single lancepyrine. The ingroup was then composed of 31 terminals, including 11 lancepyrine genera, and the trees were rooted on the outgroup scolebythid *Clystopsenella longiventris* Kieffer, 1910 (Table 1). No character from the original work was added or removed. All 69 characters were treated as unordered and non-polarized. Characters were checked using the relevant literature for *Archaepyris* Evans, 1973, *Cretepyris* Ortega-Blanco and Engel, 2013, *Liztor* Ortega-Blanco and Engel, 2013 and *Zophepyris* Engel et al., 2016. The vein Rs+M being present (53:0) in the female of *Cretepyris* and absent (53:1) in the male, this character was coded as polymorphic for that genus. The coding of *Burmapyris azevedoi* Jouault, Perrichot and Nel, 2021 and *Protopyris myanmarensis* Jouault and Nel, 2021 was done by a direct examination of the holotypes that are housed in the IGR collection.

Holopsenella Engel et al., 2016, type genus of the Holopsenellinae, has recently been excluded from Bethylidae and reclassified in its own family, as Aculeata *incertae sedis* (Lepeco and Melo 2022). In our analysis, we thus replaced *Holopsenella* by *Holopsenelliscus* Engel, 2019, a recognized Bethylidae belonging to the former 'holopsenelline' assemblage (with *Cretabythus* Evans, 1973, and *Megalopsenella* Jouault et al., 2020).

Characters of *Holopsenelliscus* were coded using the original work (Engel 2019). Phylogenetic analyses were performed in parsimony using TNT 1.5 (Goloboff and Catalano 2016). Implied-weighting and equal-weighting searches were conducted under the 'Traditional search' method, using the following parameters: space for 99 999 trees was reserved in memory, collapsing rules as Tree Bisection Reconnection and 10 000 replicates performed. For implied-weighting analyses, the setk.run script written by Salvador Arias (unpublished) was used to calculate the appropriate value of K (Goloboff et al. 2008) and returned a value of 4.375, which was subsequently used. When several trees were produced, a strict consensus was computed. To measure the robustness of the most parsimonious trees, subsequent symmetric resampling was performed for 1000 replicates. Characters were mapped on the trees using the Winclada software.

3. Systematic palaeontology

Superfamily Chrysidoidea Latreille, 1802

Family Bethylidae Haliday, 1839

Subfamily Cretabythinae subfam. nov.

Type genus. *Cretabythus* Evans, 1973.

Diagnosis. Small to mid-sized wasps (body length 2.5−7 mm); body not particularly pubescent; head prognathous; frons flat; compound eyes developed; antenna with 13 antennomeres; maxillary palpus with six palpomeres; median clypeal lobe short, not projecting; occipital carina present; dorsal pronotal area wider than long; propleuron more or less developed; prosternum concealed, nearly obscured by procoxae and propleura; anteromesoscutum with notaulus and parapsidal signum present; mesoscutellum posteriorly rounded; metanotum developed, separating mesoscutellum from metapectal-propodeal complex; metapectal-propodeal complex not elongate, without posterior spines or projections; both sexes macropterous; tegula present; fore wing with C, Sc+R, M+Cu, A, Rs+M, Rs, R1, basal segments of M and Cu tubular; [C], [R], [1Cu], [1R1], [1M] and [2R1] cells closed; [2Cu] closed in *Cretabythus*; hind wing only with C vein present; femora incrassate; tarsal claws slightly arched; metasoma without particular modifications.

Included genera. *Cretabythus* Evans, 1973, *Holopsenelliscus* Engel, 2019, *Megalopsenella* Jouault et al., 2020.

Stratigraphic extension. Lower Cenomanian to Santonian, in the deposits of northern Myanmar and Russia (Taimyr).

Table 1. Data matrix used in the phylogenetic analyses (– = inapplicable; ? = missing).

Taxa	Characters						
	1–10	11–20	21–30	31–40	41–50	51–60	61–69
Clystopsenella	2010001101	0010001000	0010000100	0010001000	1110000100	0001001010	001101100
Archaepyris	??1?0??00?	1???0??00?0	012???????	??10??????	1110010100	1101101???	00?1?0???
Azepyris	1010111200	0017??00000	01001-0020	0111001000	1110010100	1101101?01	0001?110?
Burmapyris	1010001200	1017?00000	01001-0020	0111000000	1110010100	1101101?01	0001?110?
Cretepyris	0010011220	1????0000?	??20?00?0?	??1?????00	1110010100	11(01)1101?01	??11?1?0?
Gwesped	1000111201	?01??00000	0??01-0020	0112001000	1110010100	1101101?01	0001?110?
Lancepyris	2010111210	0010100000	01001-0000	0111001000	1110010100	1101001000	101??110?
Liztor	1010011210	1017??0000?	01001-0220	0?11100?00	1110010100	111-1?1?01	?011?1???
Protopyris	2010011200	1017?00000	01001-0020	0111000000	1110010100	0101101?01	0001?110?
Paralanceis	1010101201	1017?00000	01001-0010	0111007000	1110010100	0101001?01	0001?110?
Yunbayin	2010111200	?017?00000	01001-0020	0?11007?00	1110010100	1101101?01	0001?110?
Zophepyris	1010011210	?????00001?	01001-0??0	0?1?001?00	1110010100	111-001?01	?001?110?
Pycnomesitius	2010000100	0000100010	0010001001	0111001010	1110010100	111-1-1000	101110111
Sulcomesitius	2010101120	0000100000	0010001001	2111001010	1110010100	111-1-1001	101110111
Apenesia	(02)010100111	01121(01)0000	(01)100(01)110(01)0	(02)1(01)0(01)(01)1(01)0(01)	0110010100	111-1-1001	10(01)001100
Dissomphalus	(12)010100(01)(01)	01101(01)000(01)	(01)000(01)110(01)0	(02)1(01)0(01)(01)1(01)0(01)	0110010100	111-1-1001	10(01)001100
Pristocera	(12)0101001(12)1	01001(01)0000	(01)010(01)110(01)0	21(01)0(01)(01)1(01)0(01)	0110010100	111-1-1001	(01)0(01)001100
Pseudisobrachium	(12)01010011(01)	01(01)01(01)000(01)	(01)000(01)110(02)0	(02)1(01)01(01)1(01)0(01)	0110010100	111-1-1001	10(01)0(01)1100
Bethylus	1200111110	1001200000	0101001100	1111100110	1000010110	11001-1000	111111101
Eupsenella	0210111110	0000100000	0101001100	0111000110	1100010110	0000011000	111111101
Lytopsenella	2210011110	0000100000	0101011100	0111000110	1110010110	0000011000	101111101
Sierola	2210111110	1000100000	0101011100	0111010110	1110010110	0100011000	111111101
Bakeriella	2010100110	0010100000	0000011011	0111001110	1110010110	111-1-1000	101011001
Epyris	2010100110	0000100000	0100011020	0111001110	1110010110	111-1-1000	101011001
Holepyris	1010100110	0000100000	0100011010	0111101010	1110010110	111-1-1000	101011001
Elektroepyris	2200101121	0011100000	0011011020	2112071?00	1110010100	111-1-0000	?011?1?0?
Allobethylus	1111101101	0100201000	0000011020	0112001100	1110010100	111-1-1001	001111?0?
Cephalonomia	2101111101	010(12)(23)01110	(01)0001-1110	01(01)2101(01)0(01)	00001-(01)0-0	111-1-1101	001101101
Scleodermus	2011101101	0110101110	(01)000011020	21(01)1001(01)1(01)	00001-00-0	111-1-1100	001101101
Gynopteron	2010100200	0102100000	0100011110	01110?710	1110010100	111-1-1?00	??00?0?0?
Cretabythus	201?111100	0110?0000?	01?00?7000	0110000000	1110010101	0001001?01	?011?110?
Holopsenelliscus	101?111110	?110000012	0??01-0100	0111007000	1110010100	0001001?01	101?1?110?

Remarks. As no taxonomic treatment has been provided for the leftover genera of the obsolete Holopsenellinae, i.e., *Cretabythus* Evans, 1973, *Megalopsenella* Jouault et al., 2020 and *Holopsenelliscus*, we erect the subfamily Cretabythinae. This decision is backed by our phylogenetic analyses below, where the Cretabythinae are retrieved as monophyletic yet poorly supported. An improvement of the codding and support through a revision of the three genera is strongly needed to clarify the status of the subfamily and to understand it in the modern sense of the Bethylidae. The cretabythines retain the most complete fore wing venation among the Bethylidae as their diagnostic trait, alongside other features listed above.

Subfamily Lancepyrinae Azevedo and Azar, 2012

Type genus. *Lancepyris* Azevedo and Azar, 2012.

Emended diagnosis. Small-sized wasps (body length mainly around 2−3 mm, max 5.4 mm); body black to dark castaneous, not particularly pubescent; antenna with 13 antennomeres, rarely 12; ocelli present; dorsal pronotal area elongate, narrowing anteriorly; posterior margin of dorsal pronotal area concave; mesoscuto-mesoscutellar groove present; metanotum developed medially; metapectal-propodeal complex not posteriorly produced into spines; both sexes macropterous; tegula present; fore wing with C, Sc+R, M+Cu and A tubular; Rs+M vein tubular and straight, rarely reduced to spectral; 2r-rs&Rs long, sometimes reaching anterior margin; m-cu vein sometimes present, closing [1M] cell; pterostigma large; tarsal claws slightly arched; second metasomal tergite about as long as third.

Azepyris gen. nov.

https://zoobank.org/68669837-DAC6-4EAF-8F2D-740123E127B9

Type species. *Azepyris delamarrei* **sp. nov.**

Etymology. The genus name is a combination of *Az*-, honouring both Dr. Celso O. Azevedo and Dr. Dany Azar who first named the Lancepyrinae, and -*epyris*, a suffix traditionally used to name bethylids. Gender masculine.

Diagnosis. Female. Body depressed, elongate; head longer than wide; eye elliptical, longer than high, located anteriorly on head; clypeus with median lobe projecting forward and lateral lobe not developed; mandible with three teeth, apical tooth longest; 11 flagellomeres; anterior ocellus not crossing supra-ocular line (Fig. 1A, B); mesosoma flattened; dorsal pronotal area narrow with lateral margin slightly incurved, posterior margin concave; notaulus and parapsidal signum present; mesoscuto-mesoscutellar sulcus conspicuous, reniform; mesoscutellum subquadrate, posteriorly overlapped by developed metanotum (Fig.

1C, D); metapectal-propodeal complex smooth, posterolateral corners with lateral dentiform projection (Fig. 1E); fore wing with 1Rs&1M angled at junction with Rs+M; Rs+M spectral; cu-a post-furcal to 1M; distal abscissa of R1 tubular for short distance; 2r-rs&Rs arising on distal half of pterostigma, long but not reaching wing margin (Fig. 1F); pro- and metafemora moderately thickened; proarolium well-developed (Fig. 1B); metasoma fusiform; T2 longest, laterally covering sternites (Fig. 1A, C).

Systematic remarks. Following the key to the genera of Lancepyrinae of Jouault et al. (2021), this specimen keys to *Zophepyris* due to the fore wing with Rs+M weak or spectral and cu-a post-furcal to 1M. However, *Azepyris* **gen. nov.** differs from this genus in having the head longer than wide (vs. ovoid in *Zophepyris*), the eyes elliptical (vs. rounded), the pronotum narrower, 1Rs&1M angled at junction with Rs+M (vs. straight), Rs+M nebulous to spectral but distinct (vs. absent?), the pterostigma rounded (vs. elongate), 2r-rs&Rs not fully pigmented (vs. reaching anterior wing margin), and the posterolateral corners of metapectal-propodeal complex with small projection (vs. no projections). Therefore, we propose the new genus *Azepyris* **gen. nov.** to accommodate this particular morphotype.

Azepyris delamarrei sp. nov.

https://zoobank.org/EB5CF079-C86A-4D97-9631-4B6B-CF3E52B7

Fig. 1

Etymology. The specific epithet is a patronym honouring Yann Delamarre, a student and the senior author's fellow from the palaeontology program at the University of Rennes. The specific epithet is to be treated as a noun in the genitive case.

Material studied. *Holotype* SNHM-6001, a complete female; housed in the paleontological collection of the Staatliches Naturhistorisches Museum Braunschweig, Germany (SMNH, coll. Müller).

Type locality and horizon. Hkamti site, Hkamti district, Sagaing Region, Myanmar; early Albian, ca. 110 Ma, Early Cretaceous.

Diagnosis. As for genus.

Description. Body rather depressed, elongate, poorly pubescent (length 5.35 mm). — **Head** prognathous, longer than wide; LH: 1.04 mm, WH: ca. 0.70 mm, HE: 0.60 mm, VOL: 0.20 mm; frons flat, punctate; compound eye elliptical, longer than high, not covering head length, located on anterior half of head, closer to mandible than to occipital carina; clypeus with median lobe rather projecting forward, lateral lobe poorly developed; mandible long, with three teeth, apical tooth longest; antenna fili-
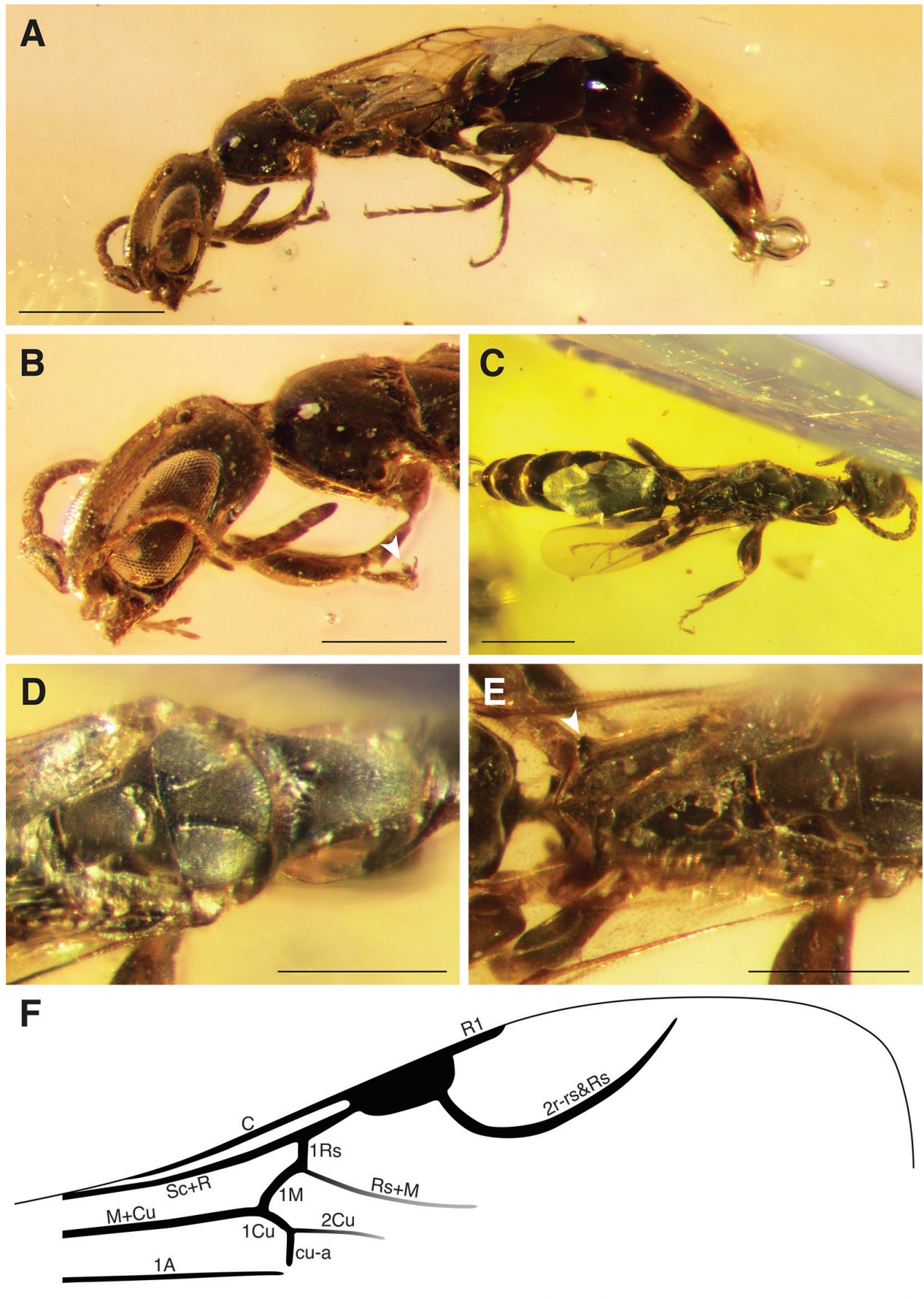
Figure 1. *Azepyris delamarrei* **gen. et sp. nov.**, holotype female number SNHM-6001. **A** habitus in lateral view; **B** head and anterior mesosoma in lateral view (arrow = fore arolium); **C** habitus in dorsal view; **D** anterior mesosoma in dorsal view; **E** posterior mesosoma in dorsal view (arrow = lateral projection of posterior corner of metapectal-propodeal complex); **F** line drawing of fore wing. Scale bars: 1 mm (A, C, F); 0.5 mm (B, D, E).

form; scape 2.17 times as long as pedicel (length 0.26 mm); flagellomeres 1−10 cylindrical, all longer than wide (length 0.09-0.10 mm); flagellomere 11 longest, tapering at apex: ocelli forming short triangle, anterior ocellus not crossing supra-ocular line; occipital carina present, complete, forming weak arch. — **Mesosoma** flattened, with dorsum smooth (length 1.62 mm); propleuron slightly visible in dorsal view, 'neck-shaped'; dorsal pronotal area 1.56 times as long as anteromesoscutum (length 0.50 mm), narrow, anterior flange developed, lateral margin slightly incurved, posterior margin concave; anteromesoscutum wider than dorsal pronotal area, posterior margin straight; notaulus deeply impressed, not reaching posterior margin of anteromesoscutum, convergent; parapsidal signum poorly marked; mesoscuto-mesoscutellar suture with reniform sulcus connecting lateral foveae; mesoscutellum subquadrate, posterior margin slightly convex; metanotum rather developed, overlapping mesoscutellum posteriorly *sensu* Azevedo et al. (2018); metapectal-propodeal complex smooth laterally, lateral marginal carina distinct, dorsal surface of metapectal-propodeal complex hardly distinguishable, apparently smooth, posterior corner with small lateral dentiform projection. Fore wing hyaline, reaching fourth metasomal segment (LFW: 2.48 mm); C, Sc+R, M+Cu, 1A tubular; 1Rs&1M angled at junction with Rs+M; Rs+M poorly pigmented, spectral; cu-a post-furcal to 1M; 2Cu pigmented, then fading; pterostigma rounded; short stub of R1 tubular distal to pterostigma: 2r-rs&Rs arising on distal half of pterostigma, long but not closing [2R1] cell. Proleg with protrochanter originating from apex of procoxa; profemur moderately thickened; tibial spur formula 1-2-2, pro- and metaspurs long, mesospurs shorter; two tarsal claws, only slightly curved; proarolium well-developed; metafemur moderately thickened; first metatarsomere as long as 2−4 combined. — **Metasoma** longer than mesosoma (length 2.69 mm); fusiform, tapering at apex; petiole conspicuous and narrow: six exposed tergites; T2 longest, laterally covering sternites; T1, T3, T4 and T5 subequal in length; short and narrow sting exserted.

Genus *Burmapyris* Jouault, Perrichot and Nel, 2021

Type species. *Burmapyris azevedoi* Jouault, Perrichot and Nel, 2021

Burmapyris ohmkuhnlei sp. nov.

https://zoobank.org/A8A54C71-153F-429B-8D71-0F9CF-9CD633B

Fig. 2

Etymology. The specific epithet is a patronym honouring Dr Christoph Öhm-Kühnle, who generously donated the specimen for study. The specific epithet is to be treated as a noun in the genitive case.

Material studied. *Holotype* IGR.BU-060, a complete female; housed in the amber collection of the Geology Department and Museum of the University of Rennes, France (IGR).

Type locality and horizon. Noije Bum, Hukawng Valley, Kachin State, northern Myanmar; late Albian-early Cenomanian, ca. 99 Ma, mid-Cretaceous.

Diagnosis. Female. Head elongate, ovoid (Fig. 2A, F); mandible small; flagellomere 1 shorter than pedicel (Fig. 2D); notaulus fully impressed (Fig. 2B); fore wing with 1Rs&1M only slightly angled at junction with Rs+M (Fig. 2C); profemur swollen; meso- and metalegs slender (Fig. 2E).

Description. Body weakly depressed and poorly pubescent (length 3.80 mm). — **Head** prognathous, elongate, ovoid; LH: 0.83 mm, WH: 0.66 mm; WF: 0.52 mm, HE: 0.23 mm; OOL: 0.31 mm; WOT: 0.10 mm; DAO: 0.05 mm; VOL: 0.43 mm; compound eye elliptical, longer than high, located anteriorly on head; clypeus with median lobe triangular, lateral lobe not developed; space between toruli depressed; antenna filiform, reaching mesoscutellum posteriorly; scape 1.73 times as long as pedicel (length 0.19 mm), dorso-ventrally flattened; 11 flagellomeres cylindrical, distinctly longer than wide except flagellomere 1 (flagellomere 1 length 0.09 mm; flagellomeres 2−10 length 0.10−0.12 mm), slightly longer than wide, shorter than pedicel; flagellomere 11 longest, tapering at apex (length 0.16 mm); mandible decussate, with four to five (?) teeth, first and second apical teeth longest, remaining shorter; ocellar triangle small, anterior ocellus posterior to supra-ocular line; occipital carina present, forming small arch posterior to ocelli. — **Mesosoma** with dorsum smooth (length 1.46 mm); propleuron only slightly visible dorsally; dorsal pronotal area narrower anteriorly, lateral margin straight, posterior margin widely concave; anteromesoscutum shorter than dorsal pronotal area, notaulus impressed on posterior two thirds of anteromesoscutum, convergent, absent anteriorly, parapsidal signum present; mesoscuto-mesoscutellar sulcus reniform, narrow; mesoscutellum posteriorly overlapped by long metanotum; metapectal-propodeal complex rectangular, without postero-lateral spine, median carina present, continuing on propodeal declivity. Fore wing hyaline, at least reaching third metasomal segment (LFW: 2.46 mm); C, Sc+R, M+Cu, 1A tubular; 1Rs&1M only slightly angled at junction with Rs+M; 1Rs shorter than 1M; 1M and cu-a aligned; Rs+M tubular, reaching apex of pterostigma; pterostigma slightly rounded; short stub of post-stigmal abscissa of R1 present; 2r-rs&Rs arising on distal half of pterostigma, long but not closing [2R1] cell; [2R1] cell large. Legs slender, only profemur swollen; tibial spur formula 1-2-2; tarsal claws slightly curved; arolium small. — **Metasoma** smooth, fusiform and elongate (length 1.51 mm); petiole short; six exposed tergites, covering sternites laterally; sting exserted.
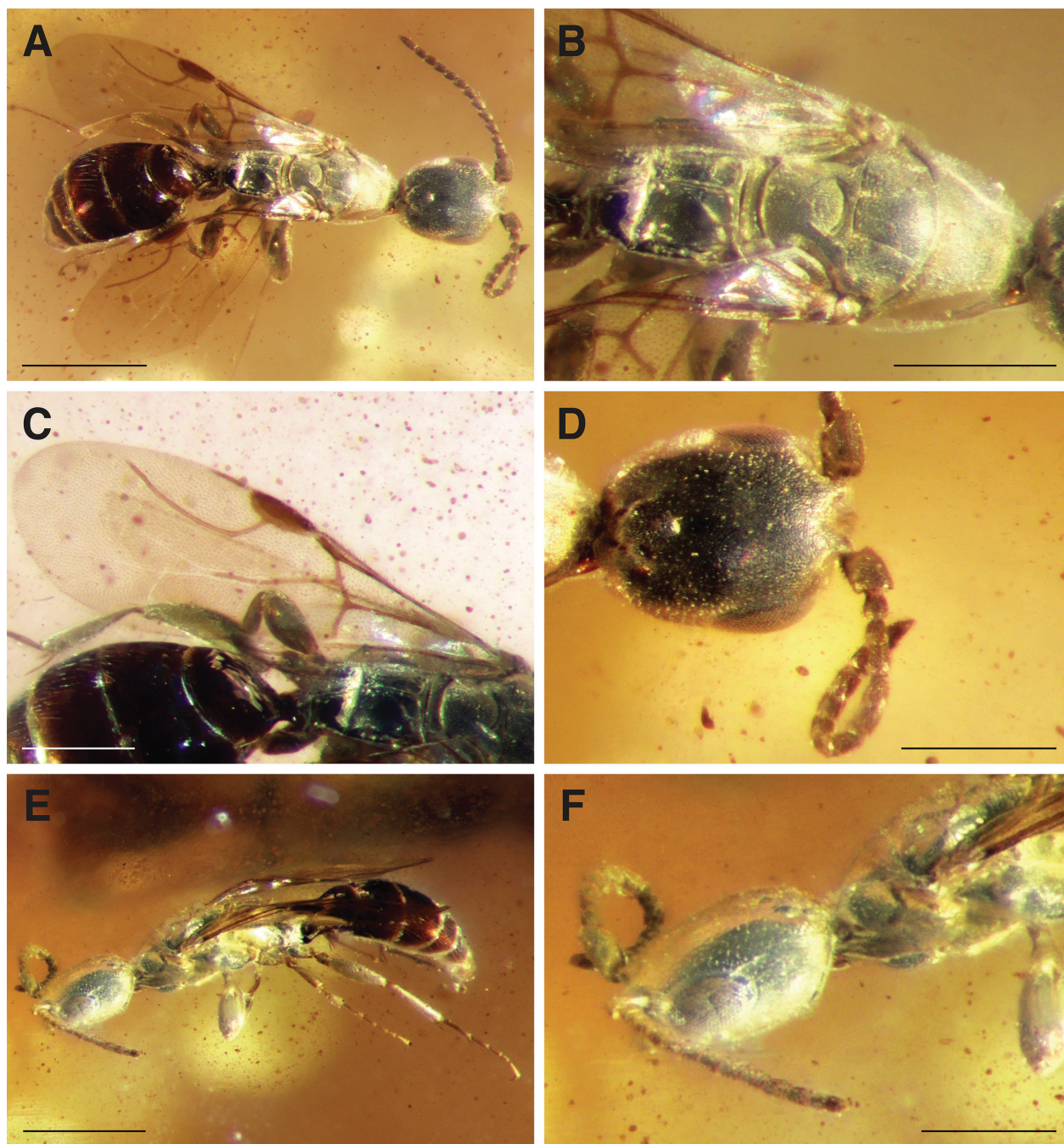
Figure 2. *Burmapyris ohmkuhnlei* **sp. nov.**, holotype female number IGR.BU-060. **A** habitus in dorsal view; **B** mesosoma in dorsal view; **C** fore wing in dorsal view; **D** head and antenna in dorsal view; **E** habitus in lateral view; **F** head and anterior mesosoma in lateral view. Scale bars: 1 mm (A, E); 0.5 mm (B, C, D, F).

Systematic remarks. Following the key to the genera of Lancepyrinae of Jouault et al. (2021), our specimen keys to *Burmapyris* Jouault, Perrichot and Nel, 2021 due to the fore wing with Rs+M vein tubular, the [2R1] cell open, the pterostigma elongate and Rs+M long, extending distally to [1M] cell, and [1M] cell not fully enclosed by tubular veins. Beside these characters, it possesses several other features reminiscent of *Burmapyris*: the general shape of the body, the very similar fore wing venation, the long antenna and the dorso-ventrally flattened scape. After reexamining the holotype of *B. azevedoi*, we noticed that it also possesses the median metapostnotal carina, strengthening the attribution of our specimen to *Burma-*

pyris. *Burmapyris ohmkuhnlei* **sp. nov.** differs from *B. azevedoi* in the shape of the head (more elongate and less rounded), the smaller mandible, the less pronounced angle of 1Rs&1M, the notaulus not fully impressed and the slender legs with only the profemur swollen.

Gwesped **gen. nov.**

https://zoobank.org/004C50ED-C52A-4DB3-976A-1DB-879CB9559

**Type species.** *Gwesped groehni* **sp. nov.**
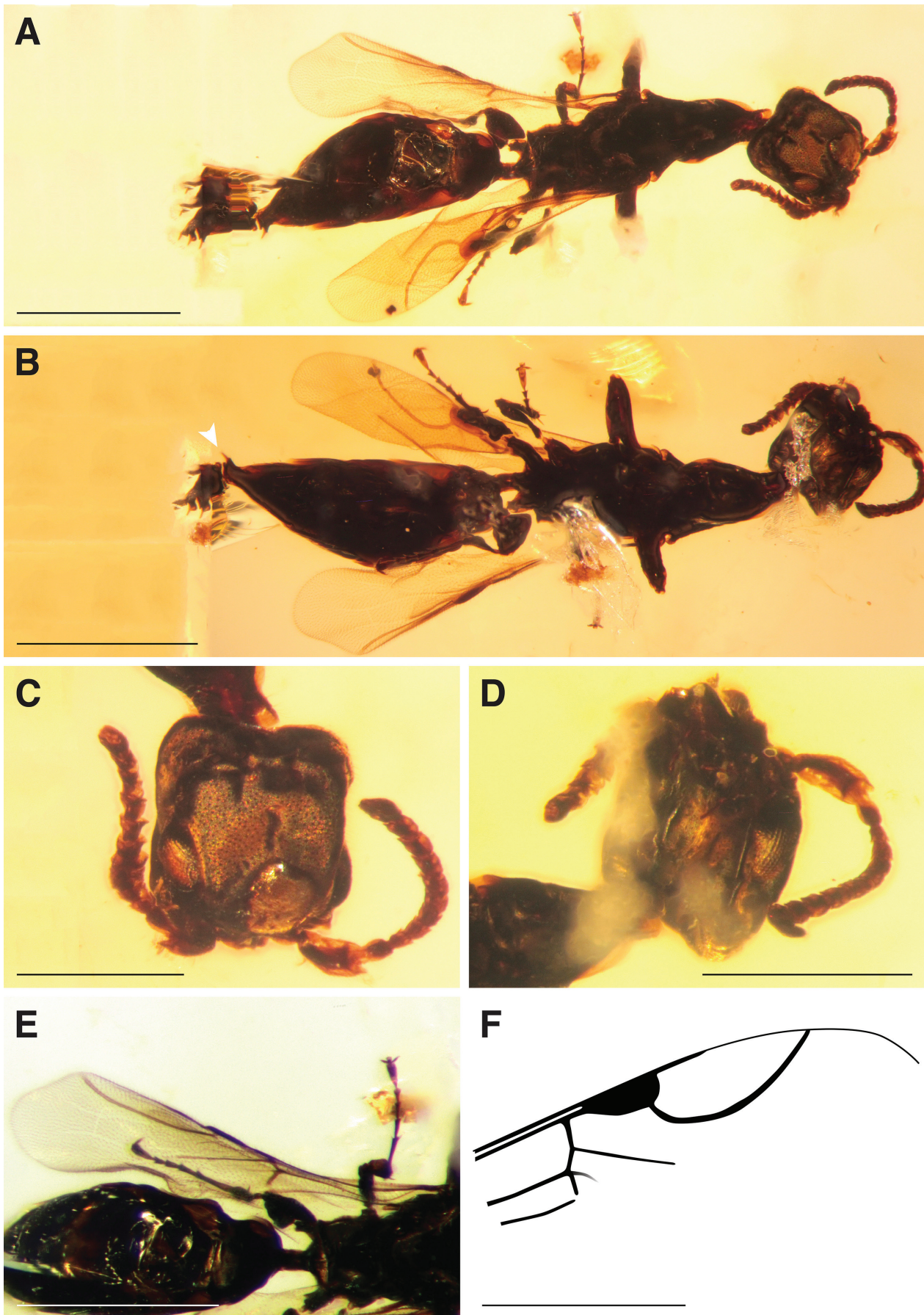
Figure 3. *Gwesped groehni* **gen. et sp. nov.**, holotype female number GPIH.5068. **A** habitus in dorsal view; **B** habitus in ventral view (arrow = sting); **C** head in dorsal view; **D** head in ventral view; **E** fore wing in dorsal view; **F** line drawing of fore wing. Scale bars: 1 mm (A, B, E, F); 0.5 mm (C, D). Note: The apparent structure at the apex of the metasoma is the result of a bubble formed in the amber, combined with some artifacts produced during the stacking process.
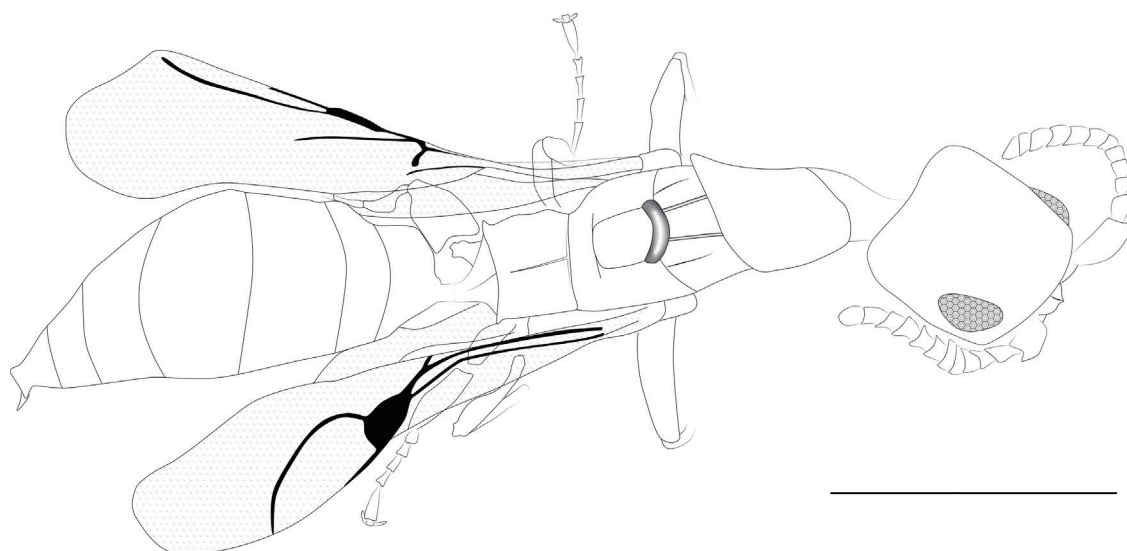
Figure 4. Line drawing of *Gwesped groehni* **gen. et sp. nov.**, holotype female number GPIH.5068. Scale bar: 1 mm.

Etymology. The genus name is taken from the word for 'wasp' in the regional Breton language (Brittany, northwestern France). Gender feminine.

Diagnosis. Female. Body flattened (Fig. 3A, B); head quadrate, about as long as wide, with metallic reflections; frons punctate; compound eye round, located on anterior half of head; antenna short; 10 flagellomeres compact (Fig. 3C, D); mesosoma narrow; propleuron visible dorsally; dorsal pronotal area narrower anteriorly; notaulus and parapsidal signum present; mesoscuto-mesoscutellar sulcus widely connecting lateral grooves; metanotum overlapping mesoscutellum posteriorly; metapostnotal median carina present; lateral margin of metapectal-propodeal complex outcurved, posterior corner with small lateral dentiform projection (Fig. 3A); fore wing with Rs+M tubular and long; pterostigma rounded; 2r-rs&Rs completely tubular (Fig. 3E, F).

Systematic remarks. Following the key to the genera of Lancepyrinae of Jouault et al. (2021), our specimen would key to *Burmapyris* due to the fore wing with Rs+M tubular, long, extending distally to [1M] cell. It differs from that genus, however, by the body generally depressed, the head quadrate, the flagellomeres compact, the fore wing with 2r-rs&Rs fully tubular and lateral dentiform projections on the posterior corners of the metapectal-propodeal complex. It differs from *Azepyris* **gen. nov.** by the head quadrate, the eyes rounded, the flagellomeres compact and the fore wing with 2r-rs&Rs completely tubular. Therefore, we propose the new genus *Gwesped* **gen. nov.** to accommodate this morphotype.

Gwesped groehni sp. nov.

https://zoobank.org/C7B02F37-05F4-4122-85FF-D54F1D8482F5

Figs 3, 4

Etymology. The specific epithet is a patronym honouring Carsten Gröhn, who generously made the specimen available for study. The specific epithet is to be treated as a noun in the genitive case.

Material studied. *Holotype* GPIH.5068, a complete female; housed in the Carsten Gröhn amber collection (under CCGG no. 11341) of the Leibniz Institute for the Analysis of Biodiversity Change, Hamburg, Germany (GPIH).

Type locality and horizon. Noije Bum, Hukawng Valley, Kachin State, northern Myanmar; late Albian-early Cenomanian, ca. 99 Ma, mid-Cretaceous.

Diagnosis. As for genus.

Description. Body depressed and poorly pubescent (length 3.82 mm). — **Head** prognathous, quadrate, about as long as wide, with metallic reflections; LH: 0.65 mm, WH: 0.56 mm; WF: 0.39 mm, HE: ca. 0.19 mm; frons flat, slightly punctate; compound eye rounded, located anteriorly on head; clypeus with median lobe only slightly projecting forward, lateral lobe poorly developed; antenna short, barely reaching pronotum posteriorly; scape 2.2 times as long as pedicel (length 0.20 mm); pedicel longer than flagellomeres 1−9; 10 flagellomeres, all compact, as long as wide; flagellomere tapering at apex, flagellomere 10 slightly longer than flagellomeres 1−9 (0.05 mm vs. 0.11 mm); occipital carina present. — **Mesosoma** narrow with dorsum smooth (length 1.56 mm); propleuron elongate, 'neck-shaped', visible dorsally; dorsal pronotal area narrower anteriorly, lateral margin slightly incurved, posterior margin straight; anteromesoscutum short, notaulus and parapsidal signum present; mesoscuto-mesoscutellar sulcus conspicuous, widely connecting lateral grooves; mesoscutellum subquadrate; metanotum developed, overlapping mesoscutellum posteriorly; metapectal-propodeal complex with metapostnotal median carina, lateral margin slightly outcurved,
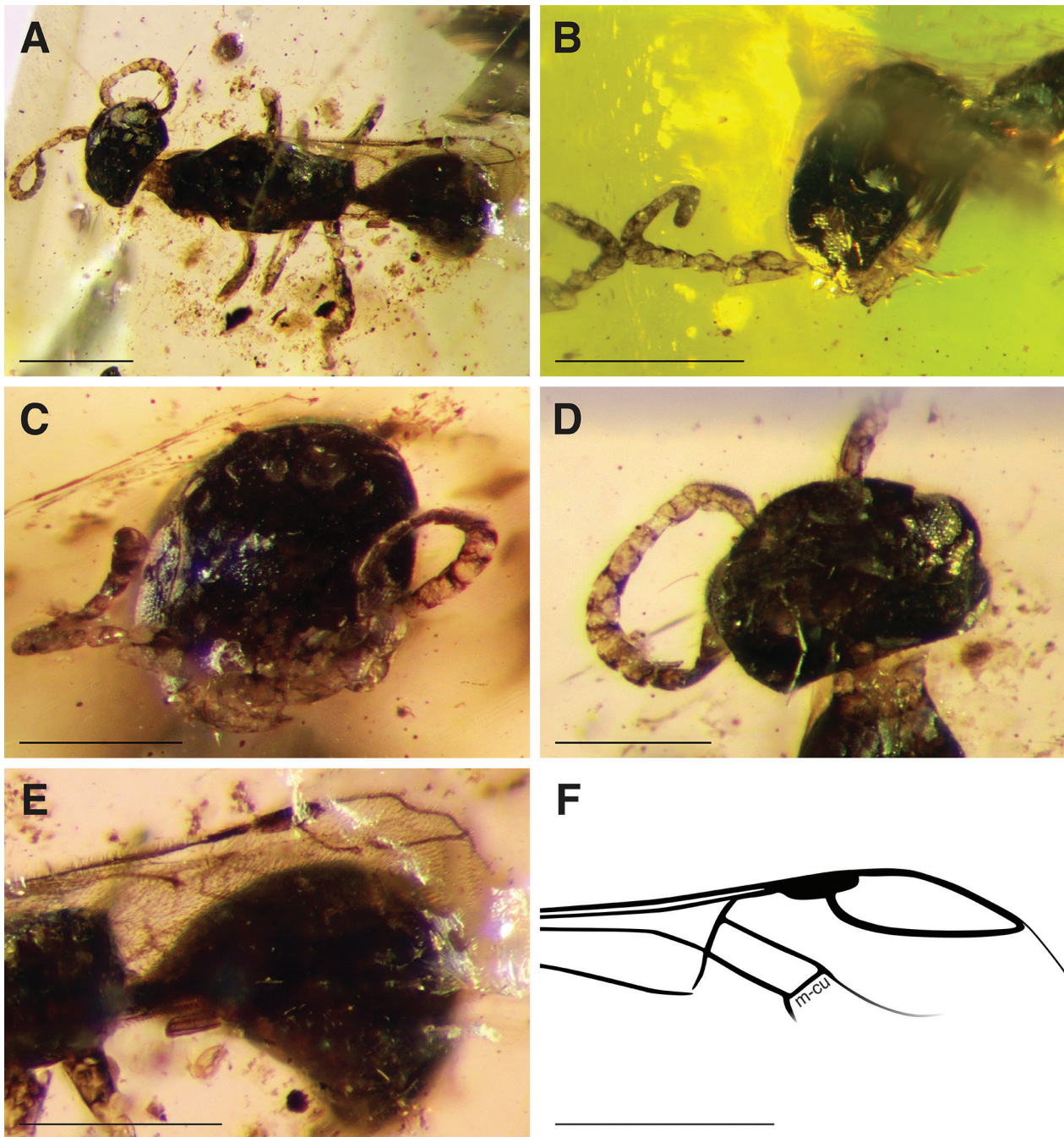
Figure 5. *Paralanceis chotardi* **gen. et sp. nov.**, holotype female IGR.BU-061. **A** habitus in dorsal view; **B** head in lateral view; **C** head in frontal view; **D** Head in ventral view; **E** fore wing and metasoma in dorsal view; **F** line drawing of fore wing. Scale bars: 1 mm (A, E, F); 0.5 mm (B, C, D).

posterior corner with small lateral dentiform projection. Fore wing hyaline, posteriorly reaching fourth metasomal segment (LFW = 2.19 mm); C, Sc+R, M+Cu, 1A tubular; 1Rs and 1M aligned; cu-a slightly post-furcal to 1M; Rs+M tubular, reaching apex of pterostigma; pterostigma rounded; 2r-rs arising from distal half of pterostigma; 2r-rs&Rs tubular, reaching wing margin; [2R1] cell large; post-stigmal abscissa of R1 tubular for half-length of [2R1] cell. Legs slender; tibial spur configuration 1-2-2; tarsal claws slightly curved; arolium small. — **Metasoma** fusiform, smooth (length 1.61 mm); petiole relatively long, conspicuous; six tergites visible, convex; short sting exserted.

Paralanceis gen. nov.

https://zoobank.org/2D119414-E742-4468-8F6F-BD-3C6B3D1BFC

Type species. *Paralanceis chotardi* **sp. nov.**

Etymology. The genus name is a combination of *Para-* and *-lanceis*, contraction of *Lancepyris*, for the similarities between the latter and the new proposed genus. Gender masculine.
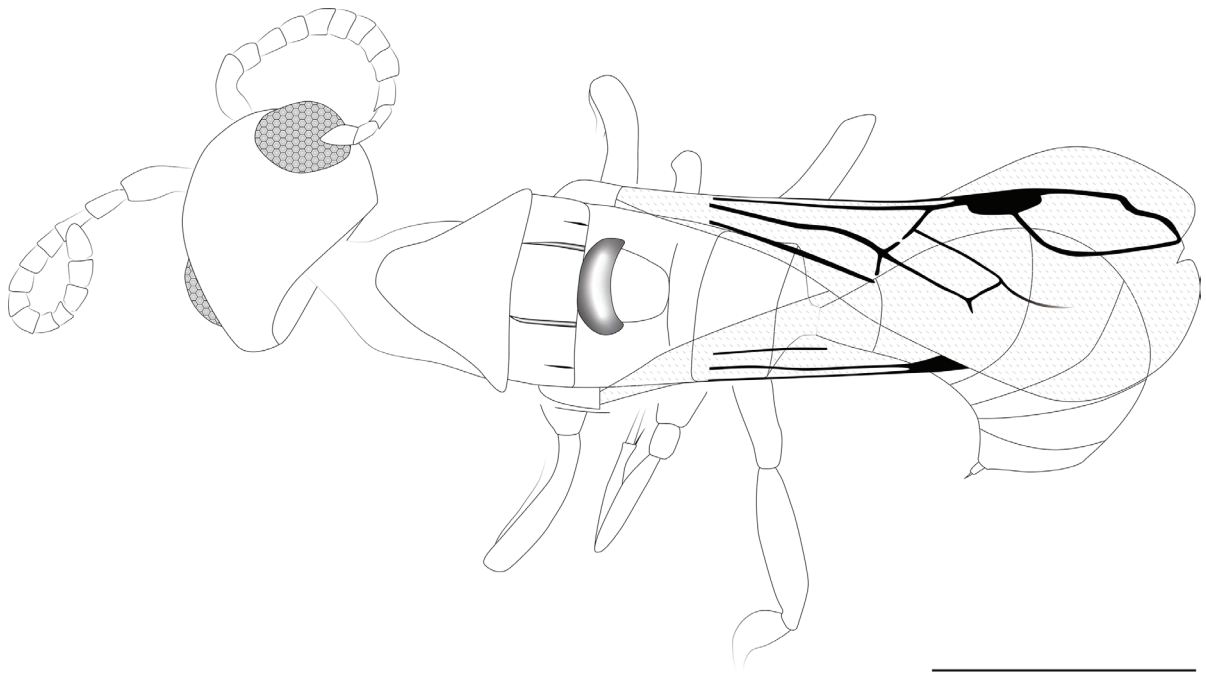
Figure 6. Line drawing of *Paralanceis chotardi* **gen. et sp. nov.**, holotype female IGR.BU-061. Scale bar: 1 mm.

Diagnosis. Female. Body stout (Fig. 5A); head ovoid; compound eye slightly longer than high, located anteriorly on head; clypeus with median lobe triangular, lateral lobe shorter; toruli separated by flat surface; antenna short; mandible with three teeth (Fig. 5B–D); propleuron elongate and visible dorsally; pronotum with lateral margin straight; metanotum long; metapectal-propodeal complex smooth, without projection (Fig. 5A); fore wing with [1M] cell elongate, fully enclosed by tubular veins; pterostigma elongate; 2r-rs&Rs arising from distal half of pterostigma; 2r-rs&Rs fully tubular; R1 tubular, closing [2R1] cell; [2R1] cell lanceolate (Fig. 5E, F).

Systematic remarks. Following the key to the genera of Lancepyrinae of Jouault et al. (2021), our specimen keys to *Lancepyris* due to the fore wing with Rs+M vein tubular and the [2R1] cell closed. It differs from this genus, however, by the head less elongate, the eyes more rounded, the space between the toruli flat, and the fore wing with [1M] cell fully enclosed by tubular veins. It also differs from *Azepyris* **gen. nov.** by the vein Rs+M tubular, the cu-a vein aligned with 1M, the [1M] cell enclosed by tubular veins and the absence of lateral dentiform projections on the posterior corners of the metapectal-propodeal complex; from *Gwesped* by the R1 vein long, distally meeting 2r-rs&Rs, the [1M] cell enclosed by tubular veins, the antennae with 11 flagellomeres and the absence of lateral dentiform projections on the posterior corners of the metapectal-propodeal complex. Compared to all the lancepyrine genera but *Lancepyris*, it is particular for possessing the [2R1] cell closed. Therefore, we propose the new genus *Paralanceis* **gen. nov.** to accommodate this morphotype.

Paralanceis chotardi sp. nov.

https://zoobank.org/C0F84EFC-D297-4303-9DD9-291417DE7F13

Figs 5, 6

Etymology. The specific epithet is a patronym honouring Matthieu Chotard, a former student and the senior author's fellow from the palaeontology program at the University of Rennes, and now working on the morphology of extinct and extant birds. The specific epithet is to be treated as a noun in the genitive case.

Material studied. Holotype IGR.BU-061, a complete female; housed in the Geology Department and Museum of the University of Rennes, France (IGR).

Type locality and horizon. Hkamti site, Hkamti district, Sagaing Region, Myanmar; early Albian, ca. 110 Ma, Early Cretaceous.

Diagnosis. As for genus.

Description. Body stout and poorly pubescent (length about 3.5 mm). — **Head** prognathous, ovoid; LH: 0.94 mm, WH: 0.74 mm; WF: 0.54 mm, HE: 0.28 mm; compound eye slightly longer than high, located anteriorly on head; clypeus with median lobe triangular and projecting forward, lateral lobe visible but much shorter than median lobe; toruli separated by flat surface; antenna filiform, short, barely reaching mesoscutellum posteriorly; scape 2.8 times as long as pedicel; 11 flagellomeres, slightly

longer than wide; flagellomere 11 longest, tapering at apex; mandibles decussate at apex, with three teeth; occipital carina present. — **Mesosoma** with dorsum smooth (length 1.80 mm); propleuron elongate and visible dorsally; dorsal pronotal area narrower anteriorly, lateral margin straight, posterior margin slightly concave; anteromesoscutum short, notaulus and parapsidal signum hardly distinguishable; mesoscuto-mesoscutellar sulcus wide, connecting lateral grooves; mesoscutellum posteriorly overlapped by metanotum; metapectal-propodeal complex smooth dorsally, rectangular, without postero-lateral spine. Fore wing hyaline, micro-pubescent (LFW: 2.40 mm); C, Sc+R, M+Cu, 1A tubular; 1Rs and 1M aligned; cu-a slightly and 1M aligned; [1M] cell elongate, fully enclosed by tubular Rs+M, m-cu and 1Cu; stub of M tubular distally to [1M] cell; stub of 2Cu visible nebulous to spectral; pterostigma elongate; 2r-rs&Rs arising from distal half of pterostigma; 2r-rs&Rs tubular, reaching wing margin; post-stigmal abscissa of R1 long, meeting 2r-rs&Rs distally; [2R1] cell closed, lanceolate. Legs slender; tarsal claws slightly incurved. — **Metasoma** fusiform, smooth; petiole short; six tergites visible, partially covering sternites laterally; tergite 2 longest; sting exserted.

Yunbayin gen. nov.

https://zoobank.org/61CB0EAA-D18F-4474-B2A9-D5AD40A862AD

Type species. *Yunbayin rossei* sp. nov.

Etymology. Yun Bayin is one of the 37 Nat spirits, a deity of the Burmese pantheon. Gender feminine.

Diagnosis. Female. Head and mesosoma depressed (Fig. 7A, E); compound eye located on anterior half of head; antenna filiform, shorter than head + mesosoma combined; flagellomeres 1−10 gradually thickening, flagellomere 10 almost as long as wide (Fig. 7A, F); dorsal pronotal area narrower than anteromesoscutum, with lateral margin incurved (Fig. 7B); anteromesoscutum half as long as dorsal pronotal area; metapectal-propodeal complex with carina; fore wing with 1Rs&1M slightly angled at junction with Rs+M and 1Rs shorter than 1M; [2R1] cell not closed, lanceolate (Fig. 7C, D); metasoma fusiform, stouter than head and mesosoma; petiole long and conspicuous (Fig. 7A, E).

Systematic remarks. Following the key to the genera of Lancepyrinae of Jouault et al. (2021), the specimens key to *Burmapyris* due to the following characters: fore wing with Rs+M vein tubular, [2R1] cell opened, pterostigma elongate and Rs+M long, extending distally to [1M] cell, [1M] cell not fully enclosed by tubular veins. However, they differ from this genus by the antenna shorter and stouter, 1Rs&1M less strongly angled, 1Rs shorter, the [2R1] cell narrower, the pronotum with lateral margin incurved, the anteromesoscutum shorter and the metasoma

not flattened and much longer than the mesosoma. They also differ from *Azepyris* **gen. nov.** by the vein Rs+M tubular and 1M aligned with cu-a; from *Gwesped* **gen. nov.** by the body less depressed, the [2R1] cell open apically, and the absence of dentiform projections of the metapectal-propodeal complex; and from *Paralanceis* **gen. nov.** by the [2R1] cell open apically and the [1M] cell not fully enclosed by tubular veins. Therefore, we propose the new genus *Yunbayin* **gen. nov.** to accommodate this morphotype.

Yunbayin rossei sp. nov.

https://zoobank.org/B68DEC44-42D4-4D15-8A12-CF7CA0E-CD1DA

Figs 7, 8

Etymology. The specific epithet is a patronym honouring Simon Rosse-Guillevic, a former student and the senior author's fellow from the palaeontology program at the University of Rennes. The specific epithet is to be treated as a noun in the genitive case.

Material studied. *Holotype* IGR.BU-062, a complete female; **paratype** IGR.BU-063, a complete female; both housed in the Geology Department and Museum of the University of Rennes, France (IGR).

Type locality and horizon. Holotype from Hkamti site, Hkamti district, Sagaing Region, Myanmar; early Albian, ca. 110 Ma, Early Cretaceous. Paratype from Noije Bum, Hukawng Valley, Kachin State, northern Myanmar; late Albian-early Cenomanian, ca. 99 Ma, mid-Cretaceous.

Diagnosis. As for genus

Description. Body weakly depressed, elongate, poorly pubescent (length 2.43 mm). — **Head** prognathous, subquadrate and longer than high; LH: 0.42 mm, WH: 0.37 mm, WF: 0.25 mm, HE: 0.21 mm, VOL: 0.12 mm; frons flat; compound eye elliptical, longer than high, not covering head length, located on anterior half of head, closer to mandible than to occipital carina; antenna filiform, shorter than head + mesosoma combined; scape 2.8 times as long as pedicel (length 0.11 mm); pedicel longer than flagellomeres 1−10, thicker (length 0.04 mm); flagellomeres elongate, longer than wide; flagellomeres 1−10 gradually thickening, flagellomere 10 almost as long as wide (length 0.03 mm); flagellomere 11 longest (length 0.06 mm), tapering at apex; at least four maxillary palpomeres; occipital carina present. — **Mesosoma** flattened, with dorsum smooth (length 0.76 mm; height 0.21 mm); propleuron elongate and visible in dorsal view; prosternum short between procoxae; dorsal pronotal area narrower than anteromesoscutum, with lateral margin incurved, posterior margin slightly concave; anteromesoscutum shorter than dorsal pronotal area, with notaulus present and convergent posteriorly, para-
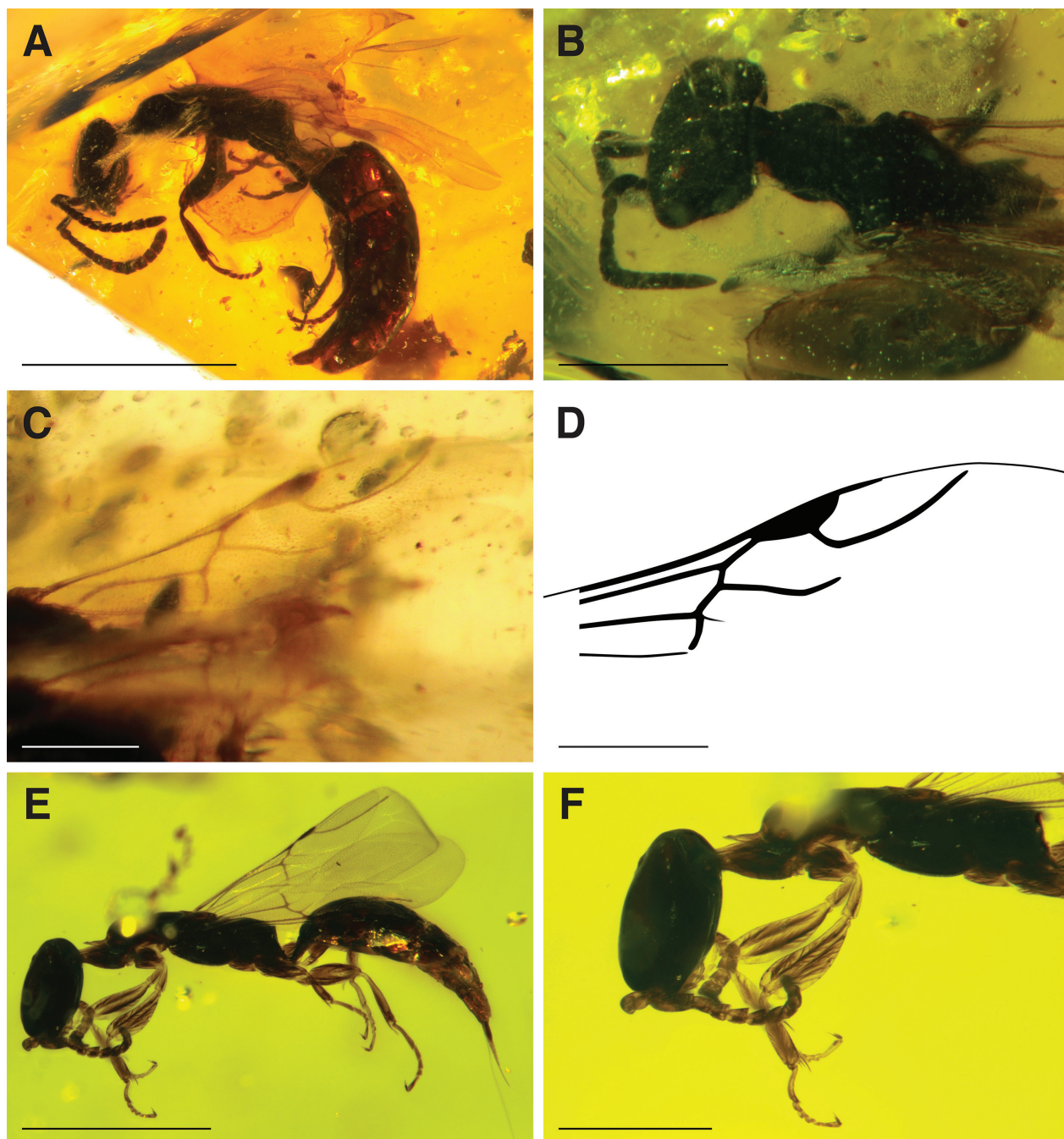
Figure 7. *Yunbayin rossei* **gen. et sp. nov.**, holotype female IGR.BU-062. **A** habitus in lateral view; **B** head and mesosoma in dorsal view; **C** fore wing in dorsal view; **D** line drawing of fore wing; paratype IGR.BU-063; **E** habitus in lateral view; **F** head and mesosoma in lateral view. Scale bars: 1 mm (A, E); 0.5 mm (B, C, D, F).

psidal signum present; scutellum posteriorly overlapped by metanotum; metapectal-propodeal complex carinate, rectangular, without posterior spine. Fore wing hyaline, reaching at least third metasomal segment (LFW: 1.39 mm); C, Sc+R, M+Cu, 1A tubular; 1Rs&1M only slightly angled at junction with Rs+M; 1Rs shorter than 1M; cu-a slightly post-furcal to 1M; Rs+M tubular, reaching apex of pterostigma; pterostigma slightly rounded and elongate; short stub of post-stigmal abscissa of R1 present; 2r-rs&Rs arising on distal half of pterostigma, long but not closing [2R1] cell; [2R1] cell narrow, lanceolate. Hind wing without apparent venation; at least three hamuli. Proleg with protrochanter originating from apex of procoxa; femora slightly enlarged; tibial spur formula 1-2-2; tarsal claws only slightly curved; arolium present, as long as claws. — **Metasoma** cylindrical, not flattened (length 1.25 mm; height 0.39 mm); petiole long and conspicuous; seven visible segments; metasomal tergites decreasing in length; ovipositor not exserted. — ***Paratype***. Similar to holotype but longer. Body length 2.92 mm; LH: 0.56 mm; fore wing with Rs+M hardly distinguishable distally but clearly tubular, reaching apex of pterostigma (LFW: 1.46 mm); proleg with internal musculature exquisitely preserved; mesosoma length 1.08 mm, height 0.27 mm; metasoma length 1.28 mm, height 0.31 mm; ovipositor exserted, long (length 0.34 mm).

A

B
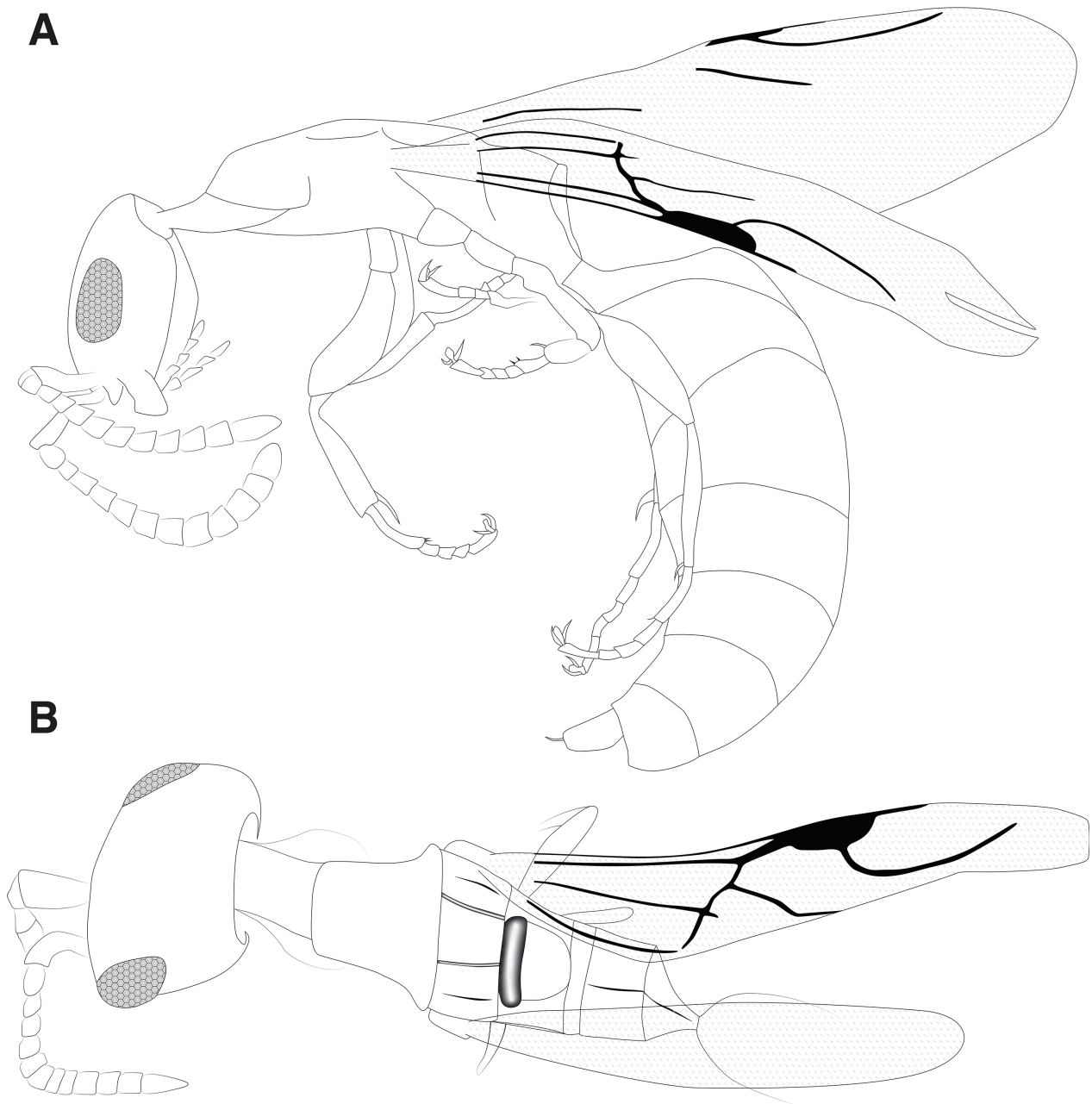
Figure 8. Line drawings of *Yunbayin rossei* **gen. et sp. nov.**, holotype female IGR.BU-062. **A** habitus in lateral view; **B** head and mesosoma in dorsal view. Scale bar: 1 mm.

Remark. Although the two specimens of the type series originate from deposits considered distinct in age, they do not show much variation. Therefore, we assign them to the same species, pending further material. To our knowledge, it is the first instance of a shared species between Hkamti and Noije Bum (Kachin) amber.

Key to the genera of Lancepyrinae
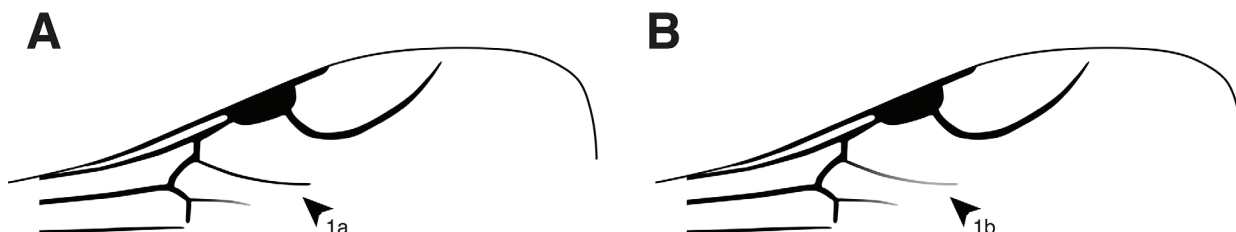
Figure 9. Schematical fore wing line drawing for characters of couplet 1. **A** Rs+M conspicuous and tubular (couplet 1a) **B** Rs+M weak (couplet 1b).

1a   Fore wing with Rs+M conspicuous and tubular (Fig. 9A) **2**
1b   Fore wing with Rs+M absent, spectral or weak (Fig. 9B) **8**
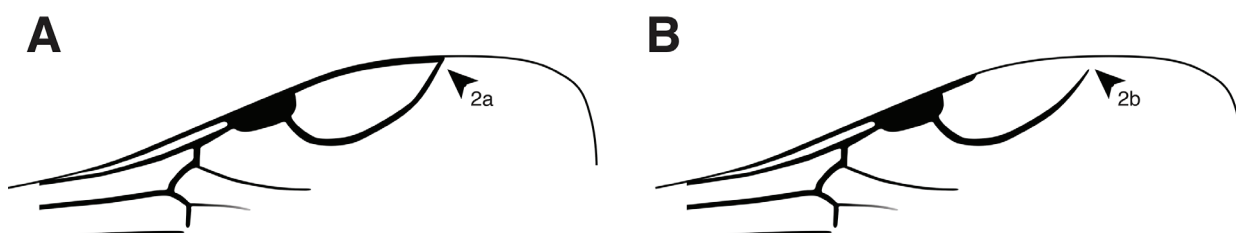
Figure 10. Schematical fore wing line drawing for characters of couplet 2. **A** [2R1] cell closed (couplet 2a); **B** [2R1] cell open (couplet 2b).

2a   Fore wing with [2R1] cell closed by 2r-rs&Rs and R1 (Fig. 10A)..**3**
2b   Fore wing with [2R1] cell open apically (Fig. 10B)..**4**
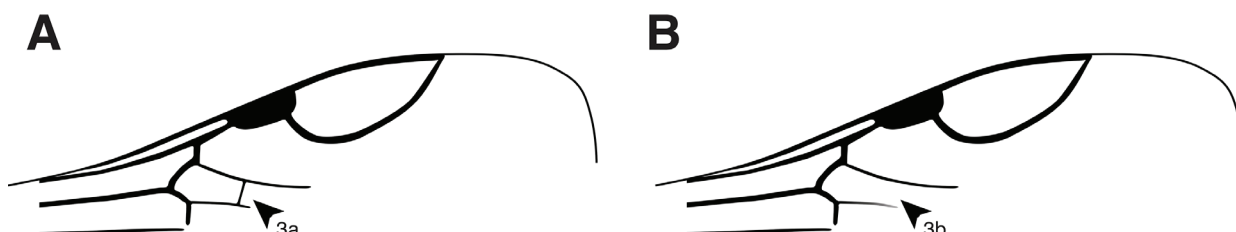
Figure 11. Schematical fore wing line drawing for characters of couplet 3. **A** [1M] cell enclosed by tubular veins (couplet 3a); **B** [1M] cell open (couplet 3b).

3a   Fore wing with [1M] cell fully enclosed by tubular veins (Fig. 11A) ....***Paralanceis* gen. nov.**
3b   Fore wing with [1M] cell open (Fig. 11B)..***Lancepyris* Azevedo and Azar, 2012**
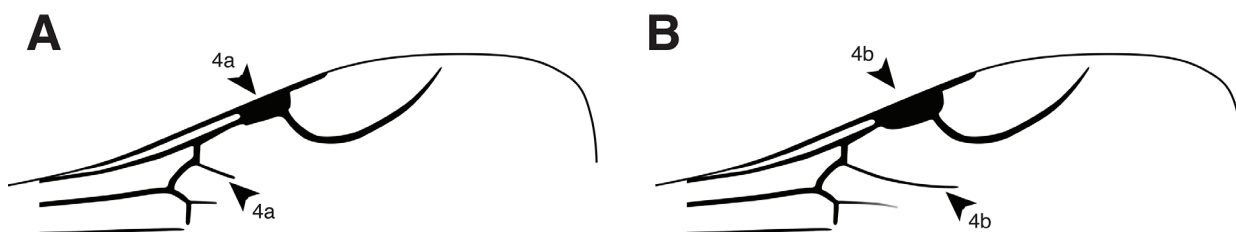
Figure 12. Schematical fore wing line drawing for characters of couplet 4. **A** Rs+M and pterostigma short (couplet 4a); **B** Rs+M and pterostigma elongate (couplet 4b).

4a   Fore wing with short pterostigma and Rs+M vein short, not enclosing [1M] cell or reaching apex of pterostigma (Fig. 12A)...***Archaepyris* Evans, 1973**
**4b**   Fore wing with elongate pterostigma and Rs+M long, enclosing [1M] cell or reaching apex of pterostigma (Fig. 12B)..**5**
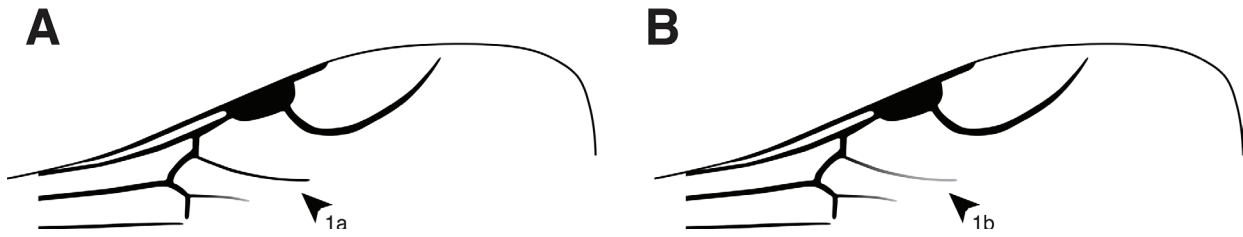
Figure 13. Schematical fore wing line drawing for characters of couplet 5. **A** [1M] cell enclosed by tubular veins (couplet 5a); **B** [1M] cell open (couplet 5b).

5a Fore wing with [1M] cell fully enclosed by tubular veins (Fig. 13A) .... *Protopyris* Jouault and Nel, 2021
**5b** Fore wing with [1M] cell open (Fig. 13B) **6**
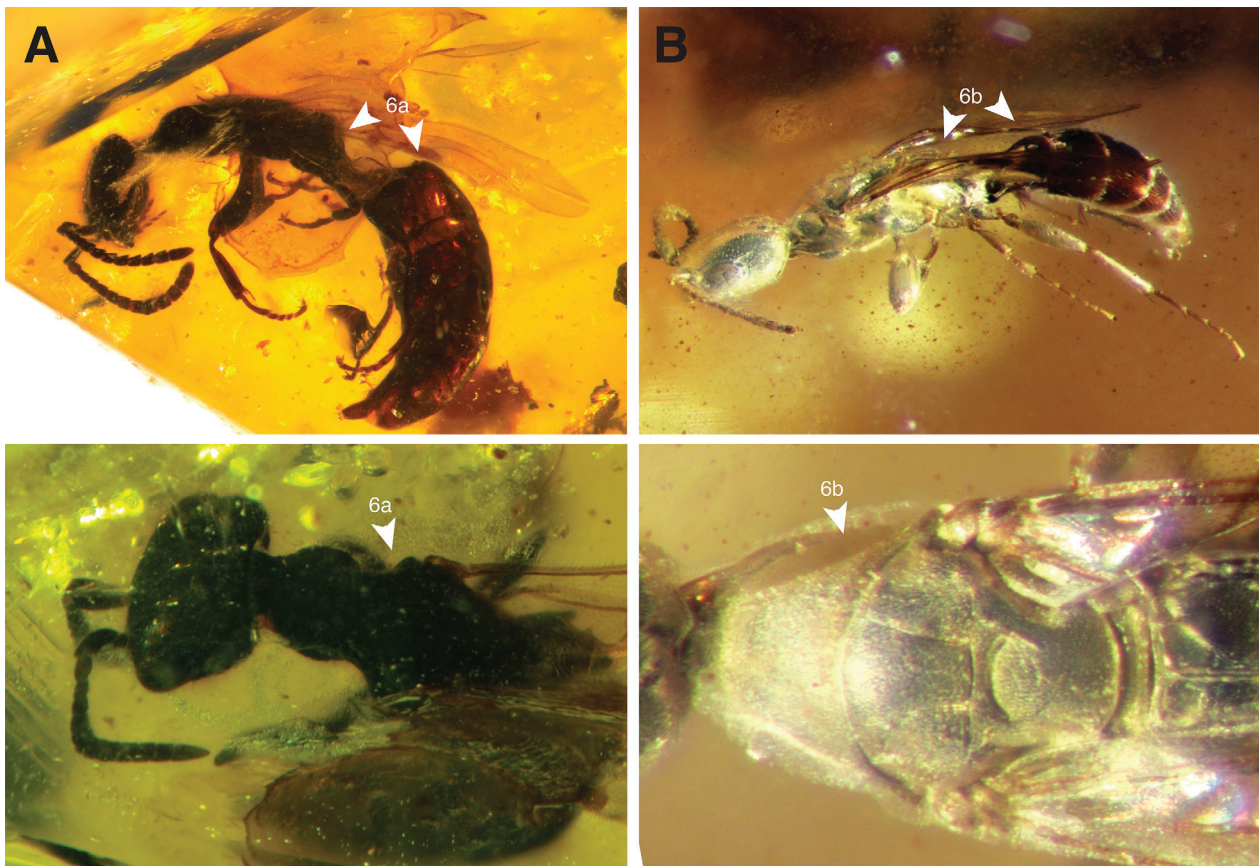
Figure 14. Pictures of head and mesosoma for characters of couplet 6. **A** top: mesosoma more flattened than metasoma, bottom: lateral margin of pronotum incurved (couplet 6a); **B** top: mesosoma as flat as metasoma, bottom: lateral margin of pronotum straight (couplet 6b).

6a Mesosoma more flattened than metasoma, lateral margin of pronotum widely incurved (Fig. 14A) ....
.... *Yunbayin* gen. nov.
6b Mesosoma equally or less flattened than metasoma, lateral margin of pronotum straight (Fig. 14B) **7**
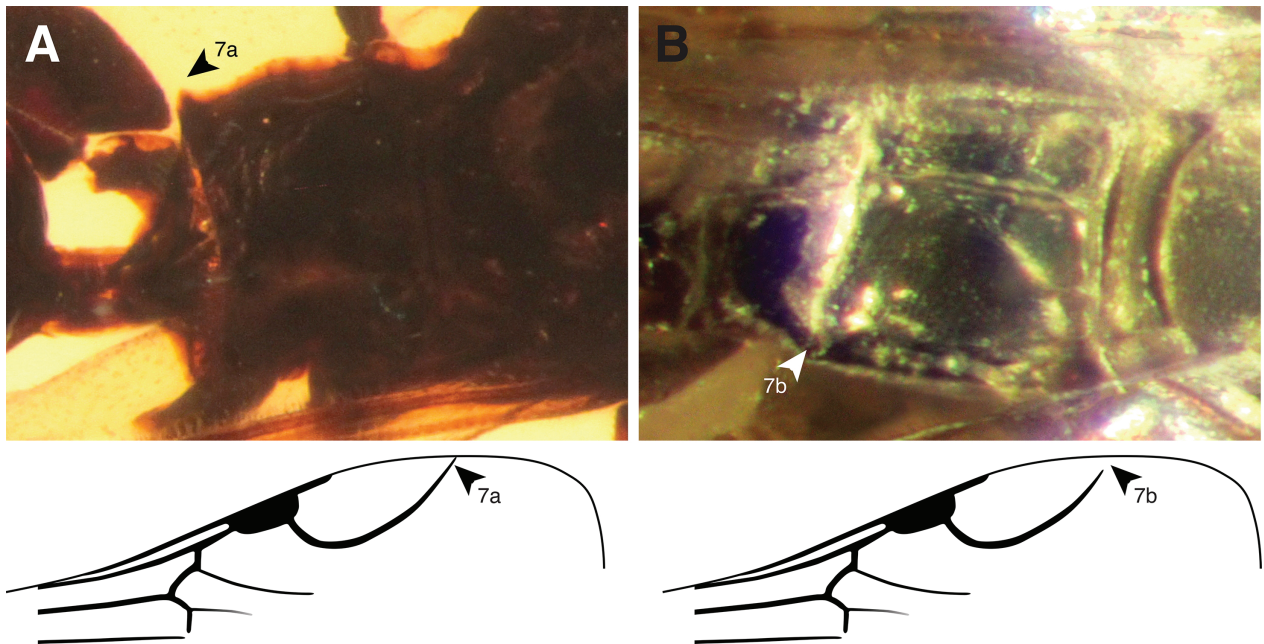
Figure 15. Pictures of metapectal-propodeal complex and schematical fore wing line drawing for characters of couplet 7. **A** top: dentiform projection of metapectal-propodeal complex, bottom: 2r-rs&Rs fully tubular (couplet 7a); **B** top: metapectal-propodeal complex without projection, bottom: 2r-rs&Rs absent distally (couplet 7b).

7a   Metapectal-propodeal complex with small dentiform projections, fore wing with 2r-rs&Rs fully tubular (Fig. 15A) ....*Gwesped* **gen. nov.**
7b   Metapectal-propodeal without such projections, fore wing with 2r-rs&Rs absent distally (Fig. 15B) ....
....*Burmapyris* **Jouault, Perrichot and Nel 2021**
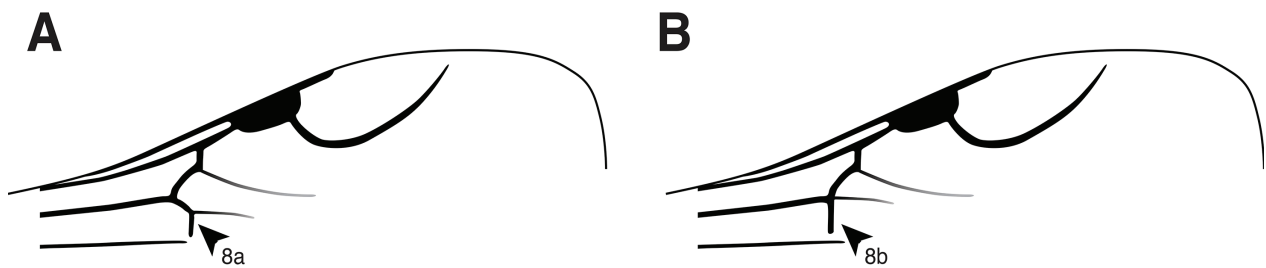
Figure 16. Schematical fore wing line drawing for characters of couplet 8. **A** cu-a post-furcal to 1M (couplet 8a); **B** cu-a aligned with 1M (couplet 8b).

8a   Fore wing with cu-a post-furcal to 1M (Fig. 16A) **9**
8b   Fore wing with cu-a aligned or antefurcal to 1M (Fig. 16B)..**10**
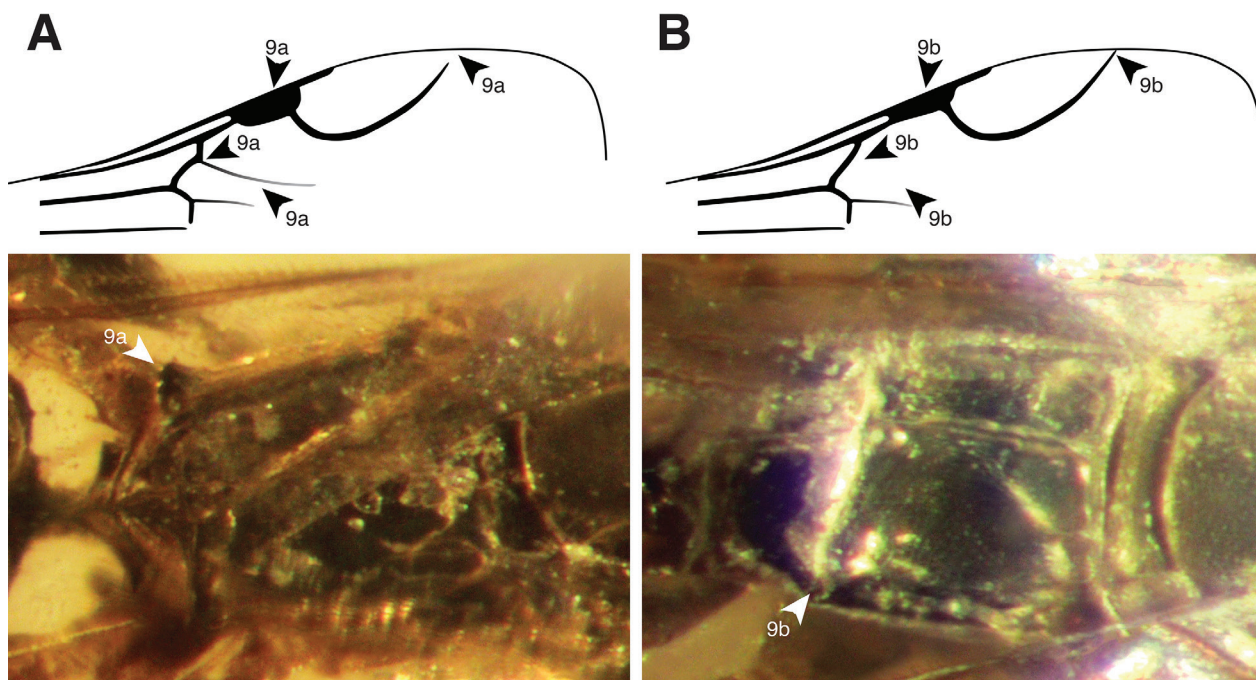
Figure 17. Schematical fore wing line drawing and pictures of metapectal-propodeal complex for characters of couplet 9. **A** top: Rs+M distinct, 1Rs&1M angled, pterostigma rounded, 2r-rs&Rs absent distally, bottom: dentiform projection of metapectal-propodeal complex (couplet 9a); **B** top: Rs+M absent, 1Rs&1M straight, pterostigma straight, 2r-rs&Rs fully tubular, bottom: metapectal-propodeal complex without projection (couplet 9b).

9a Fore wing with Rs+M weak but distinct, 1Rs&1M angled, pterostigma rounded and 2r-rs&Rs not fully tubular, metapectal-propodeal complex with small dentiform projections (Fig. 17A) ....***Azepyris* gen. nov.**
9b Fore wing with Rs+M absent, 1Rs&1M straight, the pterostigma elongate and 2r-rs&Rs fully tubular, metapectal-propodeal complex without such projections (Fig. 17B).....................................***Zophepyris* Engel et al. 2016**
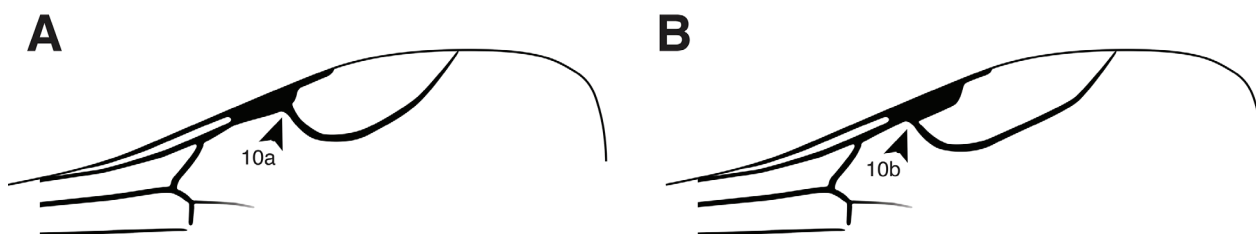
Figure 18. Schematical fore wing line drawing for characters of couplet 10. **A** 2r-rs&Rs arising distally on pterostigma (couplet 10a); **B** 2r-rs&Rs arising basally on pterostigma (couplet 10b).

10a Fore wing with 2r-rs&Rs arising on distal half of pterostigma (Fig. 18A) ....
.... ***Cretepyris* Ortega-Blanco and Engel, 2013**
10b Fore wing with 2r-rs&Rs arising on basal half of pterostigma (Fig. 18B) ....
.... ***Liztor* Ortega-Blanco and Engel, 2013**

4. Results

The search with equal weighting produced 15 most-parsimonious trees of length L = 184 steps, consistency index CI = 0.386 and retention index RI = 0.663 for 17 983 090 arrangements tried. Among those 15 trees, topological differences concerned both inter-subfamilial and intra-subfamilial relationships in the Pristocerinae, Lancepyrinae and Epyrinae. About two thirds of the trees (9/15) retrieved the Cretabythinae as the first diverging lineage and Lancepyrinae as the sister of the remaining Bethylidae. The Bethylinae were the first-diverging subfamily in the crown-group and the clade [Protopristocerinae + Epyrinae] was found to be sister to the [Mesitiinae + (Elektroepyrinae + (Scleroderminae + Pristocerinae))] clade. In the other trees (6/15), Cretabythinae were found as the first diverging lineage but the remaining subfamilies successively diverged as follows: Pristocerinae,
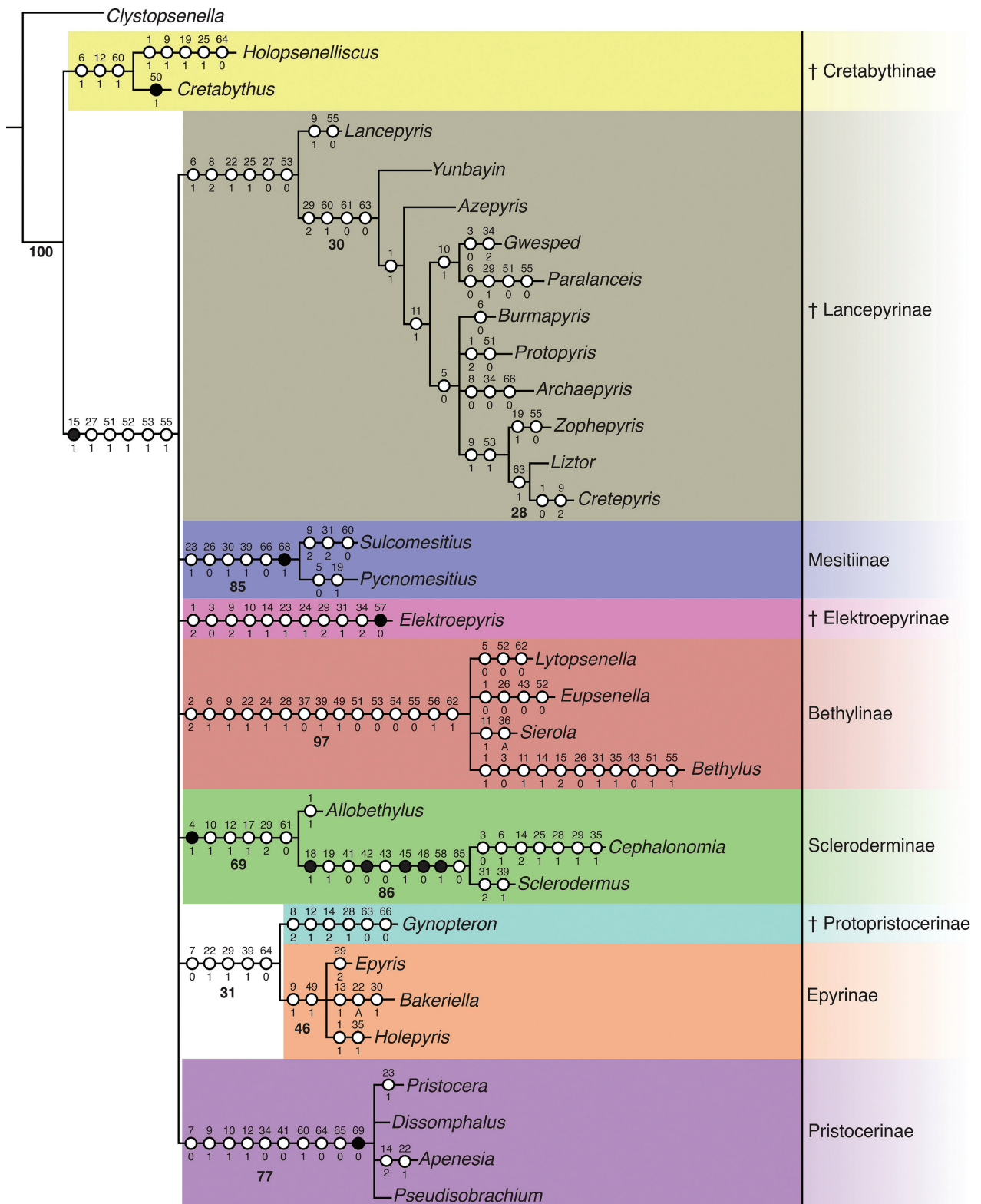
Figure 19. Strict consensus of 15 trees obtained under equal-weighting analyses. Character changes are indicated on each branch by circles, with character number and character state (as stated in Table 1) above and below circles, respectively; black circles correspond to unique changes whereas white circles indicate homoplasious character states; bootstrap support values ≥ 25 are shown below branches.

Scleroderminae, Elektroepyrinae, Mesitiinae, Proto-pristocerinae, Epyrinae, Bethylinae and Lancepyrinae. A strict consensus was computed and we obtained one cladogram (Fig. 19) of length L = 204 steps, consistency index CI = 0.348 and retention index RI = 0.603.

The search with implied-weighting produced 9 most parsimonious trees of length L = 188 steps, consistency index CI = 0.378 and retention index RI = 0.651 for 2 866 340 arrangements tried. Among those nine trees, topological differences only concerned intra-subfamilial re-
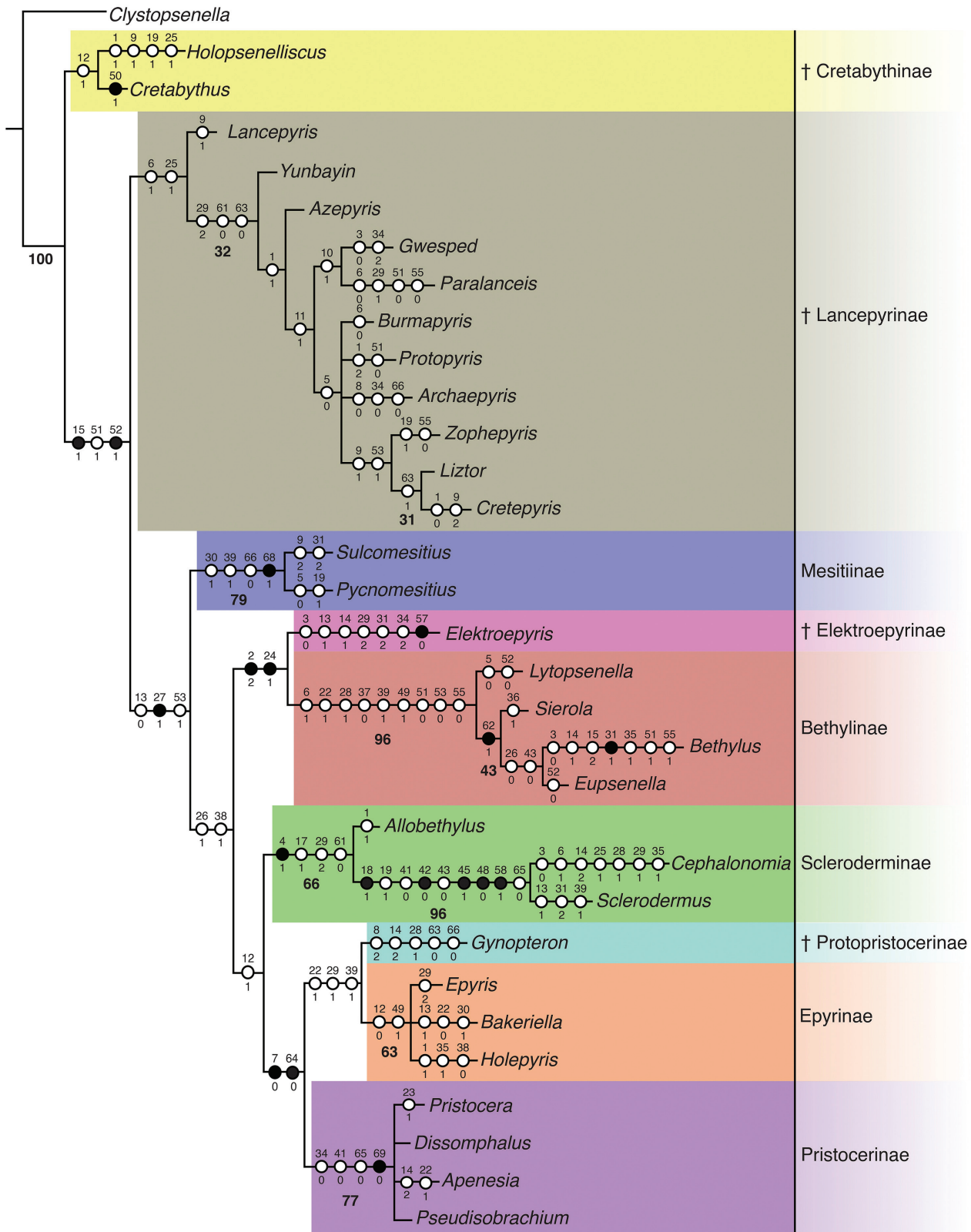
Figure 20. Strict consensus of 9 trees obtained under implied-weighting analyses. Character changes are indicated on each branch by circles, with character number and character state (as stated in Table 1) above and below circles, respectively; black circles correspond to unique changes whereas white circles indicate homoplasious character states; bootstrap support values ≥ 25 are shown below branches.

lationships in the Pristocerinae and Lancepyrinae. A strict consensus was computed and we obtained one cladogram (Fig. 20) of length L = 190 steps, consistency index CI = 0.374 and retention index RI = 0.645.

In both consensus trees, all seven non-monotypic subfamilies are retrieved as monophyletic, some being rather well-supported with bootstrap values ≥ 65 (Mesitiinae, Bethylinae, Scleroderminae, Pristocerinae and Epyrinae

under implied-weighting). Equally, the Lancepyrinae were found to be monophyletic but less strongly supported. The Lancepyrinae are supported by two characters that are common to the equal- and implied-weighting trees but neither is uniquely apomorphic for the subfamily: the scape evenly wide (6:1, also in Bethylinae and *Cephalonomia* Westwood, 1833) and the frontal line absent (25:1, also in *Holopsenelliscus*, *Cephalonomia* and Pristocerinae). The equal-weighting analyses found four additional characters supporting the monophyly of the Lancepyrinae, none being uniquely apomorphic either: the pedicel longer than wide (8:2, also in *Gynopteron* Falières and Nel, 2019 and *Pristocera* Klug, 1808), the posterior ocelli close to vertex crest (22:1, also in Bethylinae, *Gynopteron*, *Holepyris* Kieffer, 1904, *Epyris* Westwood, 1832 and *Apenesia* Westwood, 1874), the dorsal pronotal area narrow anteriorly (27:0, also in *Clystopsenella* and *Holopsenelliscus*) and the presence of the Rs+M vein of the fore wing (53:0, also in *Clystopsenella*, Cretabythinae and Bethylinae).

5.   Discussion

With hundreds of new insect species being reported each year from mid-Cretaceous Burmese amber (Ross 2022), it is not surprising to see the past diversity of an extinct or relict group revealed by the description of several new genera or species from these deposits (e.g., Selden and Ren 2017; Rasnitsyn and Öhm-Kühnle 2018; Zheng and Jarzembowski 2020). Similarly, the diversity of Lancepyrinae has increased in recent years with the discovery of new specimens. Prior to this study, only two of the seven known lancepyrine genera came from Burmese amber, a rare situation among Cretaceous Hymenoptera, given the easier access and greater quantity of Burmese Hymenoptera compared to other deposits. With the addition of four new genera and five new species, the fossil record of the Lancepyrinae is here greatly expanded. Interestingly, all but one of the genera are monospecific so that we expect many representatives of the subfamily to be discovered in the coming years. This could also be the consequence of the narrowness of the generic concepts proposed for the Lancepyrinae. However, the characters used to differentiate the different genera mainly focus on the configuration of the fore wing veins (shape or presence/absence), which is considered of generic significance in other subfamilies of Bethylidae (Azevedo et al. 2018) except for some Screlodrminae where it can vary within the same genus (e.g., Azevedo 2009).

If taxonomic boundaries between each genus are clear, this study enlightens the wide range of morphologies within the Lancepyrinae. The example of the wing venation is particularly illustrative, ranging from the simplest, with Rs+M absent and two closed cells (*Cretepyris*), to the most complete known in Lancepyrinae, with five closed cells (*Paralanceis* **gen. nov.**). Given these morphological differences, one could wonder whether they truly represent a monophyletic group, especially in the case of species with reduced or absent Rs+M vein (this vein was a diagnostic feature of the subfamily at the moment of its description). The cladistic analysis performed here confirms the positions of *Azepyris* **gen. nov.**, *Liztor*, *Zophepyris* and *Cretepyris*, which have reduced or absent Rs+M, within the Lancepyrinae. Nonetheless, the genus *Cretepyris* needs to be revised since the three type specimens of *C. martini* (plus another putative male, which is not part of the type series) show some variations (Ortega-Blanco and Engel 2013: figs 4–5) and the paratype(s) might need to be allocated to another genus or subfamily (in paratypes: Rs+M absent while stated as 'nebulose' in the holotype, [2R1] cell rounded rather than lanceolate). The genera *Liztor* and *Zophepyris* might also benefit from a more precise re-analyses to elucidate their position. Overall, and despite a lower support than for other subfamilies, the Lancepyrinae form a monophyletic group.

The four newly described genera complicate the inference of the relationships among the lancepyrine genera. While the general trend proposed for the evolution of Hymenoptera implies a simplification of the wing venation over time (Rasnitsyn 1969, 1980), such a pattern does not fit with the Lancepyrinae. Empirically, it was assumed that the most complete fore wing pattern would occur in the earliest lancepyrine, i.e., *Lancepyris opertus*, aged Barremian, and the simplest in the latest known, i.e., *Archaepyris minutus*, aged Santonian. However, the wing pattern and the age of the fossils are not fully correlated (*Paralanceis chotardi* **gen. et sp. nov.**, the representative with most complete wing venation, being as old as *Cretepyris martini*, the representative with the simplest), which suggests that the evolutionary history of the Lancepyrinae is more complex than previously thought.

Despite similar analytical parameters, our cladograms differ from that of Colombo et al. (2020). While all subfamilies are found to be monophyletic and relatively strongly supported (except for the Lancepyrinae, see below, Elektroepyrinae and Protopristocerinae, one terminal for each), their respective phylogenetic positions are not clear yet. Most of the deepest nodes of the trees are indeed poorly supported in both studies. As the equal-weighting strict-consensus tree is heavily multifurcated (except Cretabythinae, as the sister of all Bethylidae, and the Epyrinae as the sister of the Protopristocerinae, but poorly supported), we only discuss here the consensus tree found under implied-weighting analyses. The Bethylinae were previously considered as the second diverging lineage after the Holopsenellinae but are here found to be deeply nested within the family, as sister to the Elektroepyrinae with two synapomorphies (head triangular in lateral view, 2:2; ventral profile of gena angled in lateral view, 24:1). Rather than sister to the Elektroepyrinae, the Scleroderminae are retrieved as sister to a clade composed of [Pristocerinae + (Epyrinae + Protopristocerinae)]. This poorly supported clade is characterized, as in Colombo et al. (2020), by two synapomorphies (pedicel widening apically, 7:0; metapectal-propodeal complex long, 64:0). Interestingly, there is stronger sup-

port for the Epyrinae in this study than in Colombo et al. (2020; 63 vs. 44) but lower support for the clade sister to Cretabythinae (= Holopsenellinae of Colombo et al. 2020; 15 vs. 56). However, the results presented here must be interpreted with a certain degree of caution. If the morphological framework proposed by Colombo et al. (2020), the latest for the Bethylidae, has been used herein to explore the status of the Lancepyrinae subfamily, there are some limitations to its use with an extended taxonomic sampling. First, the overrepresentation of the morphologically disparate Lancepyrinae (compared to the sole *Lancepyris* used in Colombo et al. 2020) induced instabilities in the resulting trees. The sampling of *Holopsenelliscus* rather than *Holopsenella*, coded with five supplementary missing entries, also resulted in the lower support for the Cretabythinae and the clade uniting the remaining Bethylidae. Secondly, to encompass the huge morphological diversity of the family, the selection of 69 characters is for now too restrictive to reach an accurate sister-group relationship among the subfamilies. Future studies that aim to reconstruct the relationships of extant and extinct bethylid taxa should focus on expanding the character list for this purpose. Finally, several recent works have questioned the proximity of the Scolebythidae and Bethylidae, suggesting the latter to be sister to the Plumariidae (e.g., Branstetter et al. 2017; Peters et al. 2017; Melo and Lucena 2020; Jouault et al. 2020). The inclusion of the Plumariidae to the analyses might help polarizing the phylogenetic relationships within the Bethylidae but it also requires an expansion of the character sampling. Despite these limitations, it is interesting to observe the topological variations between morphological analyses and with molecular analyses.

Indeed, these morphology-based hypotheses do not fully align with molecular-based hypotheses (Carr et al. 2010; de Brito et al. 2022; Colombo et al. 2022) and many deep relationships remain undeciphered. While a sister-group relationship of Mesitiinae and Scleroderminae has been repeatedly found (Carr et al. 2010: using 'Cephalonomiini' in place of Scleroderminae; de Brito et al. 2022; Colombo et al. 2022), morphological analyses including extinct lineages retrieve the Mesitiinae in different positions [sister-group to all extant Bethylidae but Bethylinae in Colombo et al. (2020); sister-group to all extant subfamilies here]. Similarly, the Pristocerinae has been found to be sister of the Epyrinae (Carr et al. 2010: using 'Epyrini' instead of Epyrinae) or [Epyrinae + Protopristocerinae] (Colombo et al., 2020; this study), but other molecular analyses found it as sister to all extant subfamilies but the Bethylinae (de Brito et al. 2022; Colombo et al. 2022). Finally, one major change between our cladogram and those found in the above-mentioned works is the position of the Bethylinae, as the first extant subfamily to diverge in all the contributions while it is here deeply nested within the tree. The reasons that can explain these discrepancies are mainly differences in taxonomic (extant only vs. extant and extinct taxa; imbalance in the number of terminals per subfamilies) and character (molecular vs morphological) sampling. In any case, it highlights that there is still much to understand about the phylogeny of the Bethylidae, a goal that can notably be reached by extensively documenting extinct taxa and their morphologies.

6.   Conclusion

With five new species described herein, the subfamily Lancepyrinae is now composed of 12 species in 11 genera from several major deposits: Lebanese amber, Spanish amber, Myanmar amber and Taimyr amber. We confirmed the monophyly of this subfamily, while highlighting the diversity and the morphological disparity of the Lancepyrinae, and consequently of the Bethylidae, as early as the mid-Cretaceous. The relationships within the Lancepyrinae remain to be deciphered, as well as those between each subfamily, which should be achieved by combining molecular and morphological characters.

7.   Competing interests

8.   Acknowledgments

9.   References

Azevedo CO (2009) A new species of *Solepyris* Azevedo (Hymenoptera, Bethylidae) from Brazil, with amended diagnosis of the genus. Revista Brasileira de Entomologia 53: 327–330. https://doi.org/10.1590/S0085-56262009000300002

Azevedo CO, Azar D (2012) A new fossil subfamily of Bethylidae (Hymenoptera) from the Early Cretaceous Lebanese amber and its phylogenetic position. Zoologia 29: 210–218. https://doi.org/10.1590/S1984-46702012000300004

Azevedo CO, Alencar IDCC, Ramos MS, Barbosa DN, Colombo WD, Vargas JM, Lim J (2018) Global guide of the flat wasps (Hymenoptera, Bethylidae). Zootaxa 4489: 1–294. https://doi.org/10.11646/zootaxa.4489.1.1

Azevedo CO, Alencar IDCC, Ramos MS, Barbosa DN, Colombo WD, Vargas JM, Lim J (2019) Erratum: Azevedo CO, Alencar IDCC, Ramos MS, Barbosa DN, Colombo WD, Vargas JM, Lim J (2018) Global guide of the flat wasps (Hymenoptera, Bethylidae). Zootaxa: 4489(1): 001–294. Zootaxa 4559: 597–600. https://doi.org/10.11646/zootaxa.4571.4.12

Branstetter MG, Danforth BN, Pitts JP, Faircloth BC, Ward PS, Buffington ML, Gates MW, Kula RR, Brady SG (2017) Phylogenomic insights into the evolution of stinging wasps and the origins of bees and ants. Current Biology 27: 1019–1025. http://dx.doi.org/10.1016/j.cub.2017.03.027

de Brito CD, Lanes GO, Azevedo CO (2022) Morphology and evolution of the mesopleuron in Bethylidae (Hymenoptera: Chrysidoidea) mapped on a molecular phylogeny. Arthropod Structure & Development 71: 101214. https://doi.org/10.1016/j.asd.2022.101214

Carr M, Young JPW, Mayhew PJ (2010) Phylogeny of bethylid wasps (Hymenoptera: Bethylidae) inferred from 28S ans 16 rRNA genes. Insect Systematics & Evolution 41: 55–73. https://doi.org/10.1163/187631210X486995

Colombo WD, Azevedo CO (2021) Synopsis of the fossil Scleroderminae (Hymenoptera, Bethylidae) with description of a new genus and four new species from Baltic amber. Historical Biology 3: 630–638. https://doi.org/10.1080/08912963.2019.1650275

Colombo WD, Gobbi FT, Perkovsky EE, Azevedo CO (2021a) Synopsis of the fossil Pristocerinae (Hymenoptera, Bethylidae), with description of two new genera and six species from Burmese, Taimyr, Baltic and Rovno ambers. Historical Biology 33: 1736–1752. https://doi.org/10.1080/08912963.2020.1733551

Colombo WD, Perkovsky EE, Azevedo CO (2020) Phylogenetic overview of flat wasps (Hymenoptera, Bethylidae) reveals Elektroepyrinae, a new fossil subfamily. Palaeoentomology 3: 296–283. https://doi.org/10.11646/palaeoentomology.3.3.8

Colombo WD, Perkovsky EE, Waichert C, Azevedo CO (2021b) Synopsis of the fossil flat wasps Epyrinae (Hymenoptera, Bethylidae), with description of three new genera and 10 new species. Journal of Systematic Palaeontology 19: 39–89. https://doi.org/10.1080/14772019.2021.1882593

Colombo WD, Tribull M, Waichert C, Azevedo CO (2022) Integrative taxonomy solves taxonomic impasses: a case study from Epyrinae (Hymenoptera, Bethylidae). Systematic Entomology 407: 504–529. https://doi.org/10.1111/syen.12544

Cruickshank RD, Ko K (2003) Geology of amber locality in the Hukawng Valley, Northern Myanmar. Journal of Asian Earth Sciences 2: 441–455. https://doi.org/10.1016/S1367-9120(02)00044-5

Engel MS (2019) A holopsenelline wasp in mid-Cretaceous amber from Myanmar (Hymenoptera: Bethylidae). Palaeoentomology 2: 199–204. https://doi.org/10.11646/palaeoentomology.2.2.10

Engel MS, Ortega-Blanco J, Azevedo CO (2016) A new bethylid wasp in Lebanese Early Cretaceous amber (Hymenoptera: Chrysidoidea), with comments on other Mesozoic taxa. American Museum Novitates 3855: 1–14. https://doi.org/10.1206/3855.1

Evans HE (1964) A synopsis of the American Bethylidae (Hymenoptera, Aculeata). Bulletin of the Museum of Comparative Zoology 132: 1–222.

Evans HE (1973) Cretaceous aculeate wasps from Taimyr, Siberia (Hymenoptera). Psyche 80: 166–178. https://doi.org/10.1155/1973/16876

Goloboff PA, Catalano SA (2016) TNT version 1.5, including a full implementation of phylogenetic morphometrics. Cladistics 32: 221–238. https://doi.org/10.1111/cla.12160

Goloboff PA, Carpenter JM, Arias JS, Esquivel DRM (2008) Weighting against homoplasy improves phylogenetic analysis of morphological data set. Cladistics 24: 758–773. https://doi.org/10.1111/j.1096-0031.2008.00209.x

Grimaldi DA, Engel MS, Nascimbene PC (2002) Fossiliferous Cretaceous amber from Myanmar (Burma): its rediscovery, biotic diversity, and paleontological significance. American Museum Novitates 3361: 1–72. https://doi.org/10.1206/0003-0082(2002)361%3c0001:FCAFMB%3e2.0.CO;2

Harris RA (1979) A glossary of surface sculpturing. Occasional Papers in Entomology, State of California Department of Food and Agriculture 28: 1–31.

Jouault C, Ngô-Muller V, Pouillon J, Nel A (2020) New Burmese amber fossils clarify the evolution of bethylid wasps (Hymenoptera: Chrysidoidea). Zoological Journal of the Linnean Society 191: 1044–1058. https://doi.org/10.1093/zoolinnean/zlaa078

Jouault C, Perrichot V, Nel A (2021) New flat wasps from mid-Cretaceous Burmese amber deposits highlight the bethylid antiquity and paleobiogeography (Hymenoptera; Chrysidoidea). Cretaceous Research 123: 104772. https://doi.org/10.1016/j.cretres.2021.104772

Lanes GO, Kawada R, Azevedo CO, Brothers DJ (2020) Revisited morphology applied for systematics of flat wasps (Hymenoptera, Bethylidae). Zootaxa 4752: 1–127. https://doi.org/10.11646/zootaxa.4752.1.1

Lepeco A, Melo GAR (2022) The wasp genus †*Holopsenella* in mid-Cretaceous Burmese amber (Hymenoptera: †Holopsenellidae stat. nov.). Cretaceous Research 131: 105089. https://doi.org/10.1016/j.cretres.2021.105089

Martynova KV, Perkovsky EE, Olmi M, Vasilenko DV (2019) New records of Upper Eocene chrysidoid wasps from basins of Styr and Stokhod rivers (Rovno amber). Paleontological Journal 53: 998–1023. https://doi.org/10.1134/S0031030119100125

McKellar RC, Engel MS (2014) New bethylid and chrysidid wasps (Hymenoptera: Chrysidoidea) from Canadian Late Cretaceous amber. Paläontologische Zeitschrift 88: 433–451. https://doi.org/10.1007/s12542-013-0208-y

Melo GAR, Lucena DAA (2020) †Chrysobythidae, a new family of chrysidoid wasps from Cretaceous Burmese amber (Hymenoptera, Aculeata). Historical Biology 32: 1143–1155. https://doi.org/10.1080/08912963.2019.1570184

Ortega-Blanco J, Engel MS (2013) Bethylidae from Early Cretaceous Spanish amber (Hymenoptera: Chrysidoidea). Journal of the Kansas Entomological Society 86: 264–276. https://doi.org/10.2317/JKES130312.1

Peters RS, Krogmann L, Mayer C, Donath A, Gunkel S, Meusemann K, Kozlov A, Podsiadlowski L, Pedersen M, Lanfear R, Diez PA, Heraty J, Kjer KM, Klopfstein S, Meier R, Polidori C, Schmitt T, Liu S, Zhou X, Wappler T, Rust J, Misof B, Niehuis O (2017) Evolutionary history of the Hymenoptera. Current Biology 27: 1013–1018. https://doi.org/10.1016/j.cub.2017.01.027

Rasnitsyn AP (1969) The origin and evolution of Lower Hymenoptera. Trudy Paleontologicheskogo Instituta Akademii nauk SSSR 123: 1–196 [in Russian].

Rasnitsyn AP (1980) Origin and evolution of Hymenoptera. Trudy Paleontologicheskogo Instituta Akademii nauk SSSR 174: 1–192 [in Russian].

Rasnitsyn AP, Öhm-Kühnle C (2018) Three new female *Aptenoperissus* from mid-Cretaceous Burmese amber (Hymenoptera, Stephanoidea, Aptenoperissidae): Unexpected diversity of paradoxical wasps sug-

gests insular feature of source biome. Cretaceous Research 91: 168–175. https://doi.org/10.1016/j.cretres.2018.06.004

Ross AJ (2022) Supplement to the Burmese (Myanmar) amber checklist and bibliography, 2021. Palaeoentomology 5: 27–45. https://doi.org/10.11646/palaeoentomology.5.1.4

Schneider CA, Rasband WS, Eliceiri KW (2012) NIH Image to ImageJ: 25 years of image analysis. Nature Methods 9: 671–675. https://doi.org/10.1038/nmeth.2089

Selden PA, Ren D (2017) A review of Burmese amber arachnids. The Journal of Arachnology 45: 324–343. https://doi.org/10.1636/Jo-A-S-17-029

Shi G, Grimaldi DA, Harlow GE, Wang Ji, Wang Ju, Yang M, Lei W, Li Q, Li W (2012) Age constraint on Burmese amber based on U-Pb dating of zircons. Cretaceous Research 37: 155–163. https://doi.org/10.1016/j.cretres.2012.03.014

Smith RDA, Ross AJ (2017) Amberground pholadid bivalve borings and inclusions in Burmese amber: implications for proximity of resin-producing forests to brackish waters, and the age of the amber. Earth and Environmental Science Transactions of the Royal Society of Edinburgh 107: 1–9. https://doi.org/10.1017/S1755691-017000287

Yu T, Kelly R, Mu L, Ross AJ, Kennedy J, Broly P, Xia F, Zhang H, Wang B, Dilcher D (2019) An ammonite trapped in Burmese amber. Proceedings of the National Academy of Sciences of the USA 116: 11345–11350. https://doi.org/10.1073/pnas.1821292116

Zheng D, Jarzembowski EA (2020) A brief review of Odonata in mid-Cretaceous Burmese amber. International Journal of Odonatology 23: 13–21. https://doi.org/10.1080/13887890.2019.1688499

Zheng D, Chang S, Perrichot V, Dutta S, Rudra A, Mu L, Thomson U, Li S, Zhang Q, Zhang QQ, Wong Je, Wong Ju, Wang H, Fang Y, Zhang H, Wang B (2018) A Late Cretaceous amber biota from central Myanmar. Nature communications 9: 3170. https://doi.org/10.1038/s41467-018-05650-2